

Correlation-Adjusted Regression Survival Scores for High-Dimensional Variable Selection

Thomas Welchowski^{*1}, Verena Zuber², Matthias Schmid¹

¹ *Department of Medical Biometry, Informatics and Epidemiology,
University Hospital Bonn, Germany*

² *MRC Biostatistics Unit, Cambridge University, United Kingdom*

welchow@imbie.meb.uni-bonn.de, verenaz@mrc-bsu.cam.ac.uk,
matthias.schmid@imbie.uni-bonn.de

Summary

Background

The development of classification methods for personalized medicine is highly dependent on the identification of predictive genetic markers. In survival analysis it is often necessary to discriminate between influential and non-influential markers. Usually, the first step is to perform a univariate screening step that ranks the markers according to their associations with the outcome. It is common to perform screening using Cox scores, which quantify the associations between survival and each of the markers individually. Since Cox scores do not account for dependencies between the markers, their use is suboptimal in the presence highly correlated markers.

Methods

As an alternative to the Cox score, we propose the correlation-adjusted regression survival (CARS) score for right-censored survival outcomes. By removing the correlations between the

^{*}To whom correspondence should be addressed.

markers, the CARS score quantifies the associations between the outcome and the set of “de-correlated” marker values. Estimation of the scores is based on inverse probability weighting, which is applied to log-transformed event times. For high-dimensional data, estimation is based on shrinkage techniques.

Results

The consistency of the CARS score is proven under mild regularity conditions. In simulations, survival models based on CARS score rankings achieved higher areas under the precision-recall curve than competing methods. Two example applications on prostate and breast cancer confirmed these results. CARS scores are implemented in the *R* package *carSurv*.

Conclusions

In research applications involving high-dimensional genetic data, the use of CARS scores for marker selection is a favorable alternative to Cox scores even when correlations between covariates are low. Having a straightforward interpretation and low computational requirements, CARS scores are an easy-to-use screening tool in personalized medicine research.

Key words: Biomarker discovery; Breast cancer; Multi-gene signature; Personalized medicine; Prostate cancer; Survival modeling

1. Introduction

One of the key issues in personalized medicine is to identify genetic marker signatures for the planning and the prognosis of targeted cancer therapies. With more than one of three people developing some form of cancer during their lifetimes (Howlader *and others*, 2016), individualized therapies based on genetic markers are expected to play a major role in improving progression-free and overall survival of cancer patients. Among men, for example, prostate cancer is the cancer with the highest prevalence. While there are several clinical models available for predicting disease

progression, it remains a challenging task to develop molecular signatures and improve predictive accuracy of existing models (Sboner *and others*, 2010).

Since cancer research is heavily focused on time-to-event outcomes such as progression-free survival, metastasis-free survival and/or overall survival, survival analysis is one of the predominant statistical approaches to analyze data collected in clinical cancer trials. When the aim is to relate a time-to-event outcome to a set of predictors (e.g., clinical information or genetic markers), it is common to use a survival model such as the proportional hazards model by Cox. However, when data are high-dimensional (e.g., when the number of measured genetic markers exceeds the sample size), it is impossible to fit a Cox regression model including all available covariates. A solution to this problem could be to use regularized methods such as ridge-penalized Cox regression, but even these methods often break down when the number of available markers (in particular, the number of non-influential markers) is large. It is therefore common practice to carry out data-driven variable selection *before* fitting the survival model, and to include only those “influential markers” that have passed selection step.

The predominant method for variable selection in cancer research is *univariate screening*, which evaluates the associations between the outcome of a trial and each covariate separately, e.g., by computing correlation coefficients or fitting simple regression models. The coefficients of association are usually ranked by magnitude, and the most highly ranked covariates are selected for inclusion in the statistical model of interest. Fan and Lv (2008) have provided a theoretical justification for this approach by showing that univariate screening is suitable to identify influential covariates with high probabilities under mild regularity conditions. Still, a major problem of this approach is that associations between covariates are ignored, and that the set of selected markers may include many redundant markers if these are highly correlated (and hence carry

the same information regarding their associations with the outcome). While decreasing the robustness of the final statistical model, a large set of redundant markers will also cause influential markers with weaker univariate associations to be dropped from the model. This information loss is particularly problematic when the number of selected markers needs to be restricted to a small value due to sample size or cost limitations.

In survival analysis with a right-censored time-to-event outcome, univariate screening is mostly done by computing *Cox scores*, which are given by either the Z scores obtained from univariate Cox regression models or by the p-values obtained from the respective likelihood ratio or score tests. Although p-values can be corrected for multiple testing (e.g. see Benjamini and Hochberg (1995)) to identify informative covariates, Cox scores share the same disadvantages as the univariate screening methods mentioned above.

To address these problems, we consider the *correlation-adjusted regression (CAR) score* approach, which provides a criterion for variable ranking that is based on the de-correlation of covariates in linear regression. By applying a Mahalanobis-type “de-correlating” transformation to the covariates, CAR scores measure the correlations between the de-correlated variables and the continuous outcome. The set of correlation coefficients defines a ranking of the covariates, which can be used to select informative variables in the same way as with the univariate screening methods described above. As the correlation coefficients among the covariates tend to zero, CAR scores become identical to the correlations between the non-transformed covariates and the outcome. In simulations for linear regression, CAR scores were shown to outperform methods for regularized regression (boosting, lasso) with regard to their ability to correctly recover causal genetic markers and their rankings (Zuber *and others*, 2012). On the other hand, CAR scores have not been used to model time-to-event outcomes in cancer research, as an extension of the

CAR approach to right-censored data has been lacking so far.

The purpose of this paper is therefore to develop a CAR-based method for ranking high-dimensional sets of genetic marker variables in survival analysis. The resulting score, which in the following will be termed *correlation-adjusted regression survival (CARS) score*, quantifies the correlations between the log-transformed survival time $Y = \log(T)$ and the de-correlated set of covariates \mathbf{X} . We will first define a theoretical version of the CARS score on the population level (Section 2.1). Afterwards, we will provide details on the estimation of the scores from a sample of right-censored data (Section 2.2). Specifically, we will show that all relevant expressions can be estimated using inverse-probability-of-censoring (IPC) weighting techniques, as proposed by Van der Laan and Robins (2003). In Section 3, we will present the results of a simulation study that was carried out to compare the CARS approach to univariate screening based on Cox scores. In addition, we will apply CARS scores to the Swedish Watchful Waiting Cohort data (Sboner *and others*, 2010) and to a data set on invasive breast cancer (Hatzis *and others*, 2011). The results of the paper will be summarized in Section 4.

2. Methods

2.1 Full data world / population level

The main focus of survival modeling is on analyzing the effects of a set of covariates $\mathbf{x} \in \mathbb{R}^d$ on a survival time $T \in \mathbb{R}^+$. We assume that the vector $\mathbf{x} = (X_1, \dots, X_d)^\top$ has expectation $\boldsymbol{\mu}$, covariance matrix $\boldsymbol{\Sigma}$ and correlation matrix $\mathbf{P}_{\mathbf{X}}$. Similarly, we assume that the survival time T has a finite expectation μ_T and variance σ_T^2 . A popular approach to quantify the relationship between T and \mathbf{x} is the parametric accelerated failure time (AFT) model (Klein *and others*,

2013), which is based on log-transformed survival time $Y := \log(T)$ and the model equation

$$Y = \beta_0 + \mathbf{x}^T \boldsymbol{\beta} + \epsilon, \quad (2.1)$$

where $\boldsymbol{\beta} \in \mathbb{R}^d$ is a vector of regression coefficients and ϵ a noise variable. For the derivation of CARS scores we will consider the special case of log-normally distributed survival times, i.e. ϵ is assumed to follow a normal distribution with zero mean and constant variance. Then the expected squared prediction error $E((Y - \beta_0 - \mathbf{x}^T \boldsymbol{\beta})^2)$ is minimized by regression coefficients equal to

$$\boldsymbol{\beta}^* = \Sigma^{-1} \Sigma_{\mathbf{X}Y}, \quad (2.2)$$

where $\Sigma_{\mathbf{X}Y}$ is the d -dimensional vector of covariances between \mathbf{x} and Y , and the intercept

$$\beta_0^* = \mu_Y - \boldsymbol{\beta}^{*T} \boldsymbol{\mu}. \quad (2.3)$$

Model (2.1) is a Gaussian linear regression model. Therefore, in the absence of censoring, a measure of variable importance is the CAR score $\boldsymbol{\theta}$ (Zuber and Strimmer, 2011) defined by

$$\boldsymbol{\theta} = \mathbf{P}_{\mathbf{X}}^{-1/2} \mathbf{P}_{\mathbf{X},Y}, \quad (2.4)$$

where $\mathbf{P}_{\mathbf{X}} \in \mathbb{R}^{d \times d}$ is the correlation matrix of the covariates \mathbf{X} and $\mathbf{P}_{\mathbf{X},Y} \in \mathbb{R}^{d \times 1}$ is the vector of correlations between the covariates \mathbf{X} and the log-transformed survival time $Y = \log(T)$. Analogous to Cox scores, the components of $\boldsymbol{\theta}$ can be ordered by magnitude to give an importance ranking of the covariates.

The original CAR score for Gaussian linear regression can be interpreted as the correlations between the outcome variable and the de-correlated covariates, which are defined by the orthogonal transformation $\mathbf{z} = \mathbf{P}_{\mathbf{X}}^{-1/2} \mathbf{x}$ (Zuber and Strimmer, 2011). Using the best linear unbiased predictor $Y^* = \beta_0^* + \mathbf{x}^T \boldsymbol{\beta}^*$ derived from Estimators (2.2) and (2.3), and defining $\sigma_Y^2 := \text{Var}(Y)$,

the total variance of Y can be decomposed as follows:

$$\overbrace{\text{Var}(Y)}^{\text{Total variance}} = \overbrace{\text{Var}(Y^*)}^{\text{Explained variance}} + \overbrace{\text{Var}(Y - Y^*)}^{\text{Unexplained variance}} \quad (2.5)$$

$$= \sigma_Y^2 \mathbf{P}_{Y,Y^*}^2 + \sigma_Y^2 (1 - \mathbf{P}_{Y,Y^*}^2), \quad (2.6)$$

where

$$\mathbf{P}_{Y,Y^*}^2 = \mathbf{P}_{X,Y}^\top \mathbf{P}_X^{-1} \mathbf{P}_{X,Y} = \boldsymbol{\theta}^\top \boldsymbol{\theta} \quad (2.7)$$

is the squared correlation between Y and Y^* . From Equations (2.5) to (2.7) it follows that the CAR score is the central quantity to assess which variables contribute to the explained variance, or equivalently reduce the unexplained variance. Importantly, $\mathbf{P}_X^{-1/2} \mathbf{x}$ is not the Mahalanobis transform but another form of de-correlation that has the advantageous feature of maximizing the correlation between the de-correlated covariates and the standardized original covariates (Kessy *and others*, 2016). In contrast, the Mahalanobis transform maximizes the cross-covariance between the de-correlated covariates and the original covariates. Zuber and Strimmer (2011) and Zuber *and others* (2012) demonstrated that estimated CAR scores result in improved variable rankings and a high predictive performance when compared to other variable selection and modeling techniques such as lasso or boosting. Although these estimated scores work well for regression models with a continuous outcome, they were not able to deal with right-censored data so far. We will therefore develop the CAR survival (CARS) score that extends traditional estimators of CAR scores to survival modeling.

2.2 Observed data world / sample level

In the observed data world one often has to deal with right-censoring, i.e. one is no longer able to observe the uncensored survival times of all observations but only the minimum of the true survival time T and a censoring time $C \in \mathbb{R}^+$. The observed variable of interest is then defined by $\tilde{Y} = \log(\tilde{T})$, where $\tilde{T} := \min(T, C)$. Additionally, we introduce a status indicator $\Delta := \mathbf{I}(T \leq C)$,

i.e., $\Delta = 1$ if the event is observed and $\Delta = 0$ if censoring has occurred. We will further assume that T and C are independent random variables. At the sample level the empirical CAR score is defined by

$$\hat{\boldsymbol{\theta}} = \mathbf{R}_{\text{shrink}}^{-1/2} \mathbf{R}_{\mathbf{X},Y}, \quad (2.8)$$

where $\mathbf{R}_{\text{shrink}} \in \mathbb{R}^{d \times d}$ is a shrinkage estimator of the correlation matrix $\mathbf{P}_{\mathbf{X}}$ and $\mathbf{R}_{\mathbf{X},Y} \in \mathbb{R}^{d \times 1}$ is an estimator of the vector of correlations $\mathbf{P}_{\mathbf{X},Y}$. The definition of $\mathbf{R}_{\text{shrink}}$ will be provided below. In contrast to uncensored Gaussian regression, standard estimation of $\mathbf{P}_{\mathbf{X},Y}$ using the sample correlations between \mathbf{x} and \tilde{Y} is no longer appropriate, as this would result in biased estimators in the presence of right-censoring. To overcome this problem, we suggest to adjust the sample correlations by inverse-probability-of-censoring (IPC) weighting (Van der Laan and Robins, 2003), which will result in a consistent estimator of $\mathbf{P}_{\mathbf{X},Y}$.

Definition of IPC weights for right-censored data: Let $\tilde{T}_1, \dots, \tilde{T}_n$ be the observed values of \tilde{T} and C_1, \dots, C_n the underlying censoring times in a sample of i.i.d. observations of size n . Following Van der Laan and Robins (2003), we define the IPC weight of the i -th observation by

$$w_i := \frac{\Delta_i}{\hat{G}_n(\log(\tilde{T}_i))}, \quad i \in \{1, \dots, n\}, \quad (2.9)$$

where Δ_i , $i = 1, \dots, n$, are the sample values of Δ and $\hat{G}_n(\log(\tilde{T}_i))$ is an estimate of the survivor function $G(\log(T_i))$ of the logarithmic censoring process, i.e. the probability

$$G(\log(\tilde{T}_i)) = P(\log(C_i) > \log(\tilde{T}_i)). \quad (2.10)$$

By definition, censored observations ($\Delta_i = 0$) result in zero IPC weights. In line with Van der Laan and Robins (2003), we further assume that $G(\cdot) > \nu > 0$, where ν is a small positive real number (this assumption will become important in the consistency proof in Appendix A.1). To compute $\hat{G}_n(\cdot)$, we apply the Kaplan-Meier estimator to the observed logarithmic survival times

$\tilde{T}_1, \dots, \tilde{T}_n$, using the event indicators $1 - \Delta_i$, $i = 1, \dots, n$.

Estimation of the correlation vector $\mathbf{P}_{\mathbf{X},Y}$ using IPC weighting: The estimation of $\mathbf{P}_{\mathbf{X},Y}$ comprises of the following steps:

1. Estimate the expectations of the covariates X_1, \dots, X_d by their empirical means $\bar{X}_j = \sum_{i=1}^n X_{ij}/n$, $j = 1, \dots, d$, respectively, where X_{ij} denotes the sample value of the j -th covariate in observation i . Similarly, estimate the variances of X_1, \dots, X_d by their sample variances $S_j^2 = \sum_{i=1}^n (X_{ij} - \bar{X}_j)^2 / (n - 1)$, $j = 1, \dots, d$.
2. Estimate the expectation of Y by the weighted mean

$$\bar{Y}_w = \frac{1}{n} \sum_{i=1}^n w_i \log(\tilde{T}_i) , \quad (2.11)$$

where w_i , $i = 1, \dots, n$ are the IPC weights defined in Equation (2.9). Similarly, estimate the variance of Y by

$$S_{Y;w}^2 = \frac{1}{n} \sum_{i=1}^n w_i \left(\log(\tilde{T}_i) - \bar{Y}_w \right)^2 . \quad (2.12)$$

3. The covariance of X_j and Y is again estimated by IPC weighting:

$$S_{X_j,Y;w} = \frac{1}{n} \sum_{i=1}^n w_i (X_{ij} - \bar{X}_j) \left(\log(\tilde{T}_i) - \bar{Y}_w \right) , \quad j = 1, \dots, d. \quad (2.13)$$

4. The final step is to compute the empirical correlation vector $\mathbf{R}_{\mathbf{X},Y}$ by combining the estimators defined in Steps 1 to 3 above:

$$\mathbf{R}_{\mathbf{X},Y} = \left(\frac{S_{X_j,Y;w}}{\sqrt{S_{X_j}^2} \sqrt{S_{Y;w}^2}} \right)_{j=1,\dots,d} . \quad (2.14)$$

Estimation of the correlation matrix $\mathbf{P}_{\mathbf{X}}^{-1/2}$: Since the data values of the covariates are not affected by censoring, the usual sample variance-covariance estimators could be applied to obtain

an estimate of $\mathbf{P}_{\mathbf{X}}^{-1/2}$. In the presence of high-dimensional data, however, these estimators usually break down. For example, the estimation of the $d \times d$ correlation matrix $\mathbf{P}_{\mathbf{X}}$ – or more precisely its inverse square root – is challenging when d is much larger than the sample size (Edgar *and others*, 2002; Kolesnikov *and others*, 2014). We therefore propose to employ a shrinkage correlation estimator (Schäfer and Strimmer, 2005; Zuber and Strimmer, 2011) to estimate $\mathbf{P}_{\mathbf{X}}$, which is given by

$$\mathbf{R}_{\text{shrink}} = \lambda \mathbf{I}_d + (1 - \lambda) \mathbf{R}_{\mathbf{X}}, \quad (2.15)$$

where $\lambda \in \mathbb{R}^+$ is a shrinkage parameter, \mathbf{I}_d is the identity matrix of dimension $d \times d$, and $\mathbf{R}_{\mathbf{X}}$ is the matrix containing the empirical bivariate sample correlations of the covariates. Following Schäfer and Strimmer (2005), we define $\lambda := \sum_{j \neq k} \widehat{\text{Var}}(r_{j,k}) / \sum_{j \neq k} r_{j,k}^2$, where $r_{j,k}$ denotes the sample correlation between the j -th and the k -th covariate. The inverse square root $\mathbf{R}_{\text{shrink}}^{-1/2}$ can be computed very efficiently by applying a singular value decomposition of the sample correlation matrix. For details, we refer to Zuber and Strimmer (2011) and Kessy *and others* (2016). The estimation of $\mathbf{P}_{\mathbf{X},Y}$ described above, combined with the shrinkage estimator $\mathbf{R}_{\text{shrink}}$, defines the CARS score in Equation (2.8).

Consistency of CARS scores: Next we give a sketch of the consistency proof for the estimated CARS score $\hat{\boldsymbol{\theta}} = \mathbf{R}_{\text{shrink}}^{-1/2} \mathbf{R}_{\mathbf{X},Y}$. As shown in detail in Appendix A.4, $\hat{\boldsymbol{\theta}}$ converges to its population value $\boldsymbol{\theta} = \mathbf{P}_{\mathbf{X}}^{-1/2} \mathbf{P}_{\mathbf{X},Y}$ as $n \rightarrow \infty$, provided that (i) censoring is independent of the survival times, and (ii) the Kaplan-Meier estimator \hat{G}_n is a consistent estimator of G . More specifically, by embedding the IPC-weighted expressions given in the Estimators (2.11) to (2.14) in the framework of unbiased estimating equations (Huber, 1967; Carroll and Ruppert, 1988), we show that each of the estimators contained in the definition of $\hat{\boldsymbol{\theta}}$ is a consistent estimator of its respective population variance or covariance. As a consequence, $\hat{\boldsymbol{\theta}}$ results in a consistent estimator of the population value $\boldsymbol{\theta}$.

Variable selection based on CARS scores: As shown above, CARS scores measure the associations between the de-correlated covariates and the time-to-event outcome T . Variable selection can therefore be carried out by ranking the CARS scores according to their absolute values. A set of covariates is selected whose absolute CARS scores exceed the pre-defined threshold value ϕ . A suitable threshold can, for example, be obtained by cross-validating the multivariable survival model that incorporates the selected covariates. In this paper, we will use a computationally less expensive strategy and apply the adaptive false discovery rate density approach proposed by Strimmer (2008), which assumes a two-component discrete mixture model of “influential” and “non-influential” covariates. Based on this model, a suitable threshold value ϕ can be estimated by a tradeoff between the false-non-discovery rate $P(\text{“influential”} | \theta \leq \phi)$ and the false-discovery rate $P(\text{“not-influential”} | \theta \geq \phi)$. The associated parameters of the mixture model are estimated by penalized maximum likelihood and a modified semi-parametric Grenander estimator (Grenander, 1956; Strimmer, 2008). For details, and also for an overview of the advantages of the approach, we refer to Strimmer (2008).

3. Results

3.1 *Design of the simulation study*

To analyze the performance of CARS scores, we compared the CARS-based screening approach to a univariate screening approach using Cox scores (Fan and Lv, 2008). With the latter approach, a univariate Cox model was fitted for each covariate, and the Cox scores were given by the standardized coefficients of these models. In addition, we fitted multivariable Cox regression models with L_1 -penalized coefficients (Simon *and others*, 2011). In these models, a variable was considered to be “included” in the model when its L_1 -penalized coefficient estimate differed from zero. To ensure a fair comparison with the other methods, no tuning of the regularization parameter

was applied, as this would have required additional test data. Instead we used the median value of the default L_1 norm regularization path computed by the *R* (R Core Team, 2017) package *glmnet* (Simon *and others*, 2011).

We considered three sample sizes ($n \in \{250, 500, 1000\}$) and three dimensions of the covariate space ($d \in \{500, 1000, 2000\}$). The covariate values were generated from a multivariate normal distribution with zero mean. For the covariance structure of the multivariate normal distribution, a block correlation structure with three equally sized blocks was constructed. In the first block, 50% of the correlations were set to $\rho = -0.25$, and the other 50% were set to $\rho = 0.25$. In the second block, 50% of the correlations were set to $\rho = 0.5$ and the other 50% to $\rho = -0.5$, and in the third block, 50% of the correlations were set to $\rho = 0.75$ and the other 50% to $\rho = -0.75$. The correlation between covariates belonging to different blocks was zero. To satisfy the restrictions of a correlation matrix (e.g. positive definiteness) the closest correlation matrix with regard to quadratic elementwise differences was computed. Further details on the algorithm for the construction of the correlation matrix are given in the Appendix B.4.

The percentages of influential covariates that were related to the time-to-event outcome was varied according to the values 1%, 5%, and 10%. Two different correlation scenarios were analyzed: In the first scenario all influential variables were taken from the first block of the correlation matrix (“scenario with low absolute correlations”), and in the second scenario all influential variables were taken from the third block (“scenario with high absolute correlations”). The survival process was assumed to follow a log-normal distribution $T \sim \log N(\log \mu_T, \log \sigma_T^2)$ with expectation $\log \mu_T = \mathbf{X}\boldsymbol{\beta}$. The coefficients $\boldsymbol{\beta}$ were specified to be equidistant within the interval $[-0.9, 1]$, depending on the number of influential covariates. The variance $\log \sigma_T^2$ was adjusted such that explained variances of $\{25\%, 50\%, 75\%\}$ were achieved on the log-scale. The censoring process was

also assumed to be log-normally distributed. Its parameters were adjusted such that censoring rates of 0.25 and 0.75 were obtained. All values of the observed times that were higher than their empirical 90% quantile were cut off and were set to be censored. For each of the scenarios we carried out 300 independent simulation runs.

To evaluate the performance of the methods, the covariates selected by CARS scores, Cox scores and L_1 penalized Cox regression were compared to the sets of influential variables having a true (non-zero) effect on the survival times. For each threshold of the CARS and Cox scores, these comparisons resulted the cross-tabulation of the binary variables “selected vs. non-selected” and “influential vs. non-influential”. In the case of L_1 penalized Cox regression variables with coefficients greater than zero were defined as selected and all other variables as non-selected. Since we were interested in detecting a small set of influential markers within a sparse modeling framework, we used the area under the precision-recall curve (PR-AUC, Rijsbergen 1979) to evaluate the cross tables and to measure the performance of the three methods. In addition, we investigated the ability of the methods to rank the variables - from least to most important - by analyzing the rank correlations between the true absolute coefficients and the corresponding estimated absolute CARS or Cox scores.

3.2 *Scenario with low absolute correlations and low censoring rate*

The results of the scenario with low absolute correlations (first block of the correlation matrix, $\rho = \pm 0.25$) and with 25% censoring rate are presented in this section. After running the algorithm for the construction of the correlation matrix (presented in Appendix B.4), all correlations had absolute values that were smaller than 0.3. Figure 1 shows the summary of all simulations results regarding sample size n and number of covariates d . The median of CARS scores was higher than both Cox score approaches in most combinations of n and d . In addition Figure 2 displays

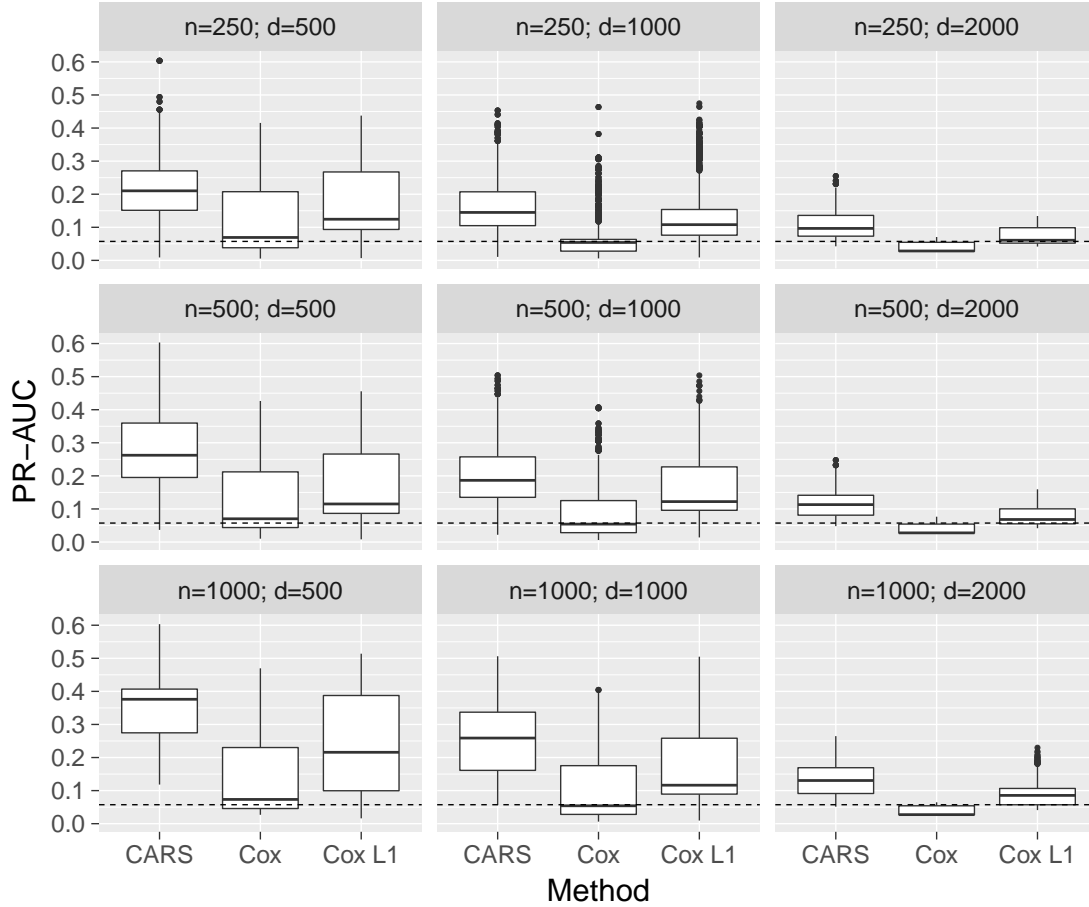


Fig. 1. Simulation: PR-AUC of CARS, Cox and Cox L_1 scores stratified by sample size (n) and number of covariates (d) with low absolute covariate correlations ($\rho = \pm 0.25$) and low censoring rate of 25%. Each boxplot summarizes the results of 2700 simulation runs (3 explained variance ratios \times 3 signal to noise ratios \times 300 repetitions).

the results with respect to the relative number of influential variables (relVar) and the explained variance (expVar). In most cases CARS scores had again higher median PR-AUC performance, except for the two upper right cases relVar = 0.01 with expVar = 0.5 or expVar = 0.75. Higher signal to noise ratios increased the performance of CARS on average. The PR-AUC of CARS scores had the largest variability compared to the Cox approaches. L_1 penalized Cox scores showed larger variability of PR-AUC than Cox scores. Further CARS scores ranked influential variables better in the median than Cox scores, as shown in Figure 3. An overall summary is

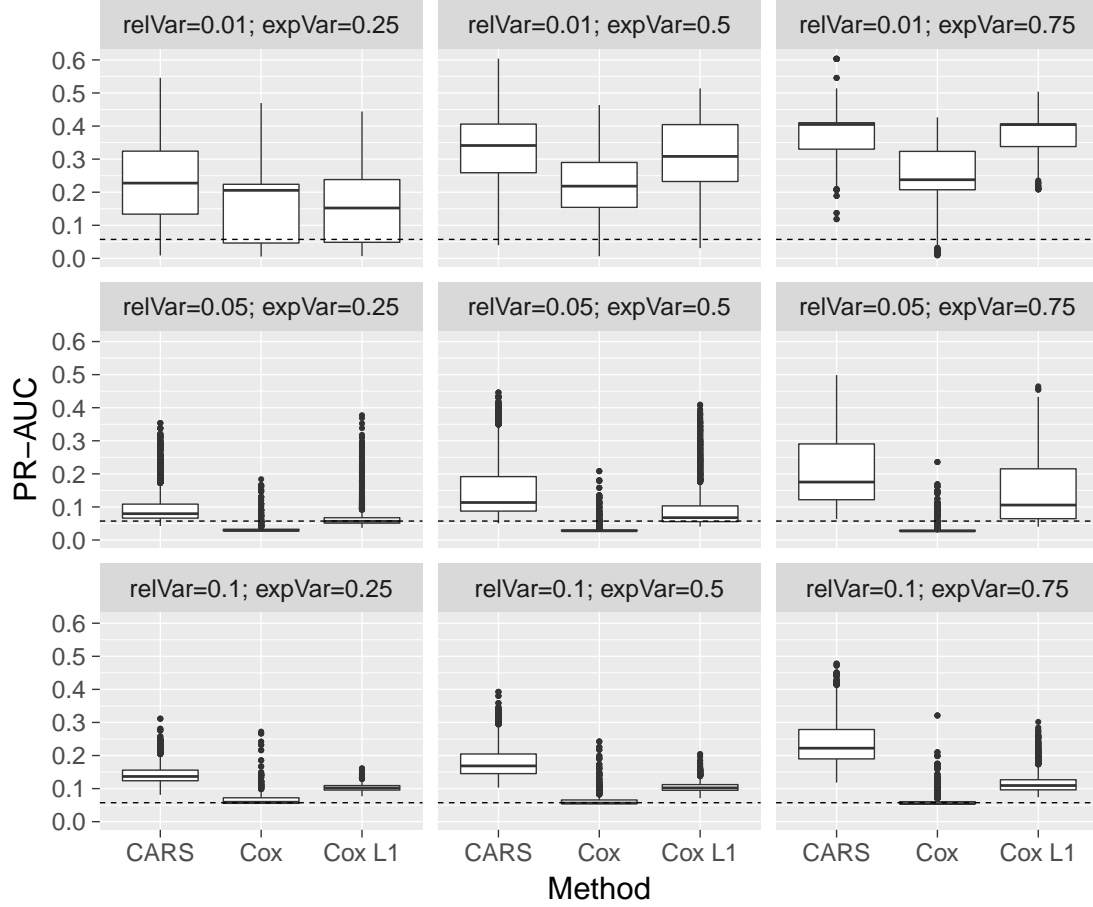


Fig. 2. Simulation: PR-AUC of CARS, Cox and Cox L_1 scores stratified by relative number of relevant variables (relVar) and explained variance (expVar) with low absolute covariate correlations ($\rho = \pm 0.25$) and censoring rate of 25%. Each boxplot summarizes the results of 2700 simulation runs (3 sample sizes x 3 number of covariates x 300 repetitions).

available in Figure 13 in the appendix.

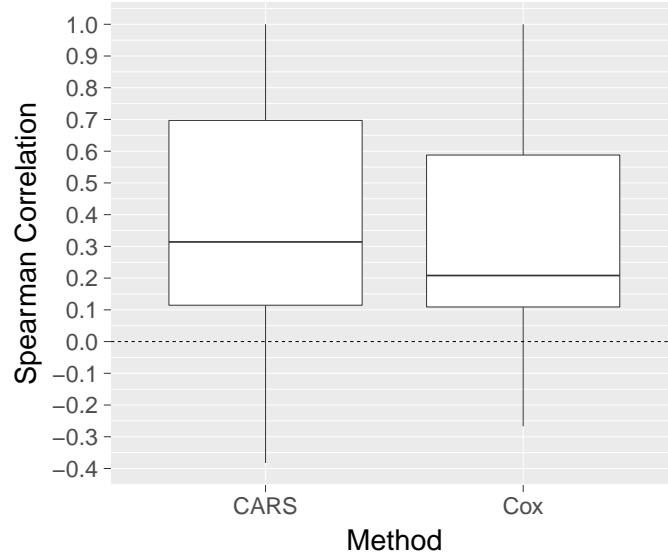


Fig. 3. Simulation study – scenario with low absolute correlations ($\rho = \pm 0.25$): This boxplot visualizes the rank correlations of the estimated and the true covariate orderings, as obtained from variable selection by CARS scores, Cox scores and L_1 -penalized Cox regression. The censoring rate was equal to 25% and low absolute covariate correlations $\rho = \pm 0.25$. Each boxplot shows the results of 24300 simulation runs (3 explained variance ratios x 3 signal to noise ratios x 3 sample sizes x 3 number of covariates x 300 repetitions).

3.3 Scenario with high absolute correlations and low censoring rate

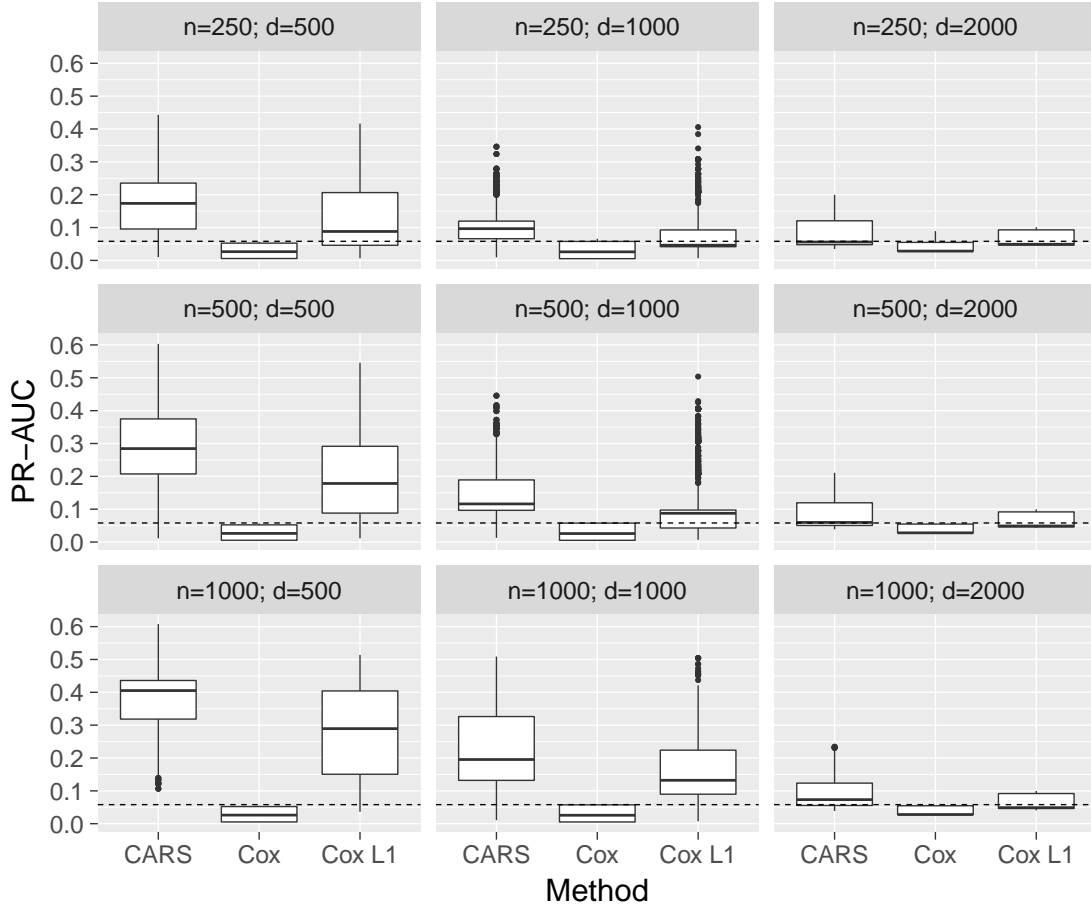


Fig. 4. Simulation: PR-AUC of CARS, Cox and Cox L_1 scores stratified by sample size (n) and number of covariates (d) with high absolute covariate correlations $\rho = \pm 0.75$ and censoring rate of 25%. Each boxplot shows the results of 2700 simulation runs (3 explained variance ratios \times 3 signal to noise ratios \times 300 repetitions).

Figure 4 presents the results of the scenario with high absolute correlations (third block of the correlation matrix, $\rho = \pm 0.75$) and with a censoring rate of 25% regarding sample size n and number of covariates d . The median of CARS scores was higher than both Cox score approaches for most combinations of n and d . However the PR-AUC performance of Cox scores decreased in comparison to the low correlation $\rho = 0.25$ scenario. Figure 5 displays the results

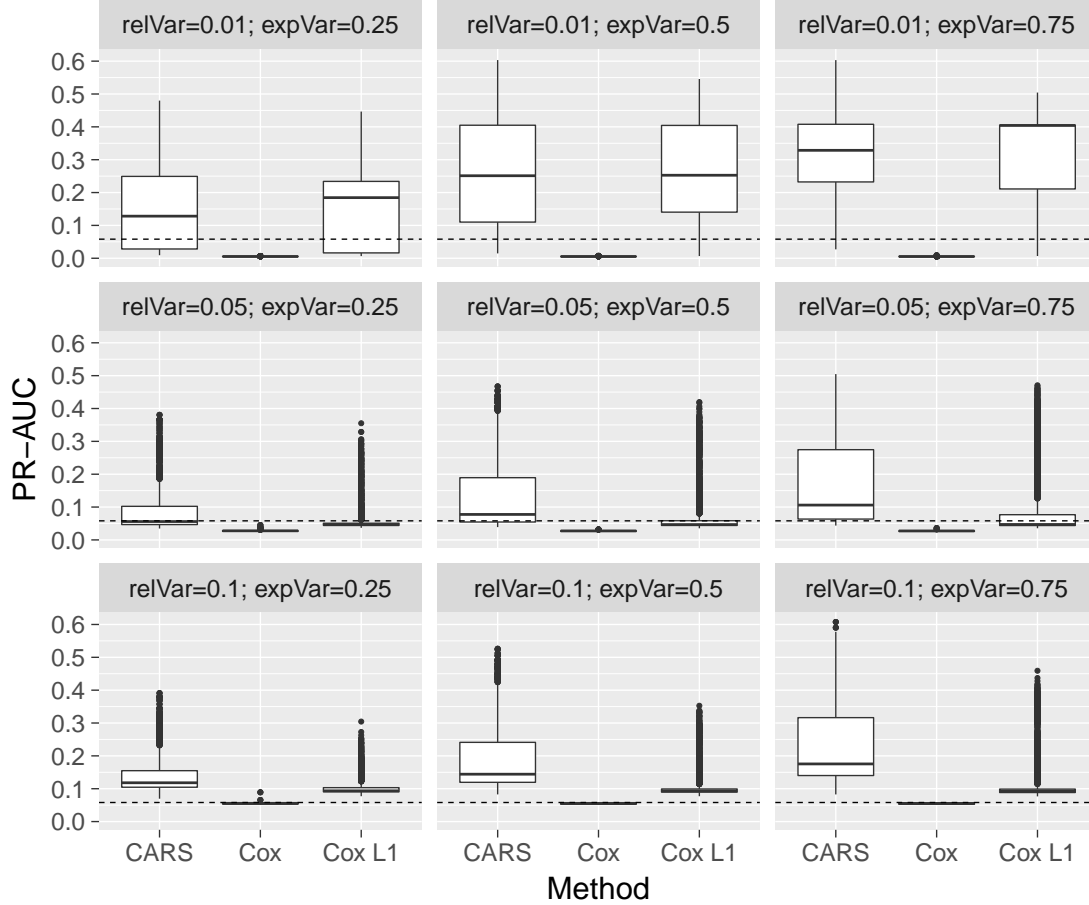


Fig. 5. Simulation: PR-AUC of CARS, Cox and Cox L_1 scores stratified by relative number of relevant variables (relVar) and explained variance (expVar) with high absolute covariate correlations $\rho = \pm 0.75$ and censoring rate of 25%. Each boxplot shows the results of 2700 simulation runs (3 sample sizes x 3 number of covariates x 300 repetitions).

with respect to the number of influential variables and the explained variances. If $\text{relVar} > 0.05$ CARS scores had again higher median PR-AUC performance than both Cox score approaches. The lack of adjustment for between-covariate correlations degraded performance of Cox scores. This effect propagated to the rank correlation (Figure 6); in particular, the gap between median rank correlations of CARS and Cox scores had become larger compared to the low correlation scenario (Figure 3). The Figure 4 in the appendix shows a summary of all simulations results.

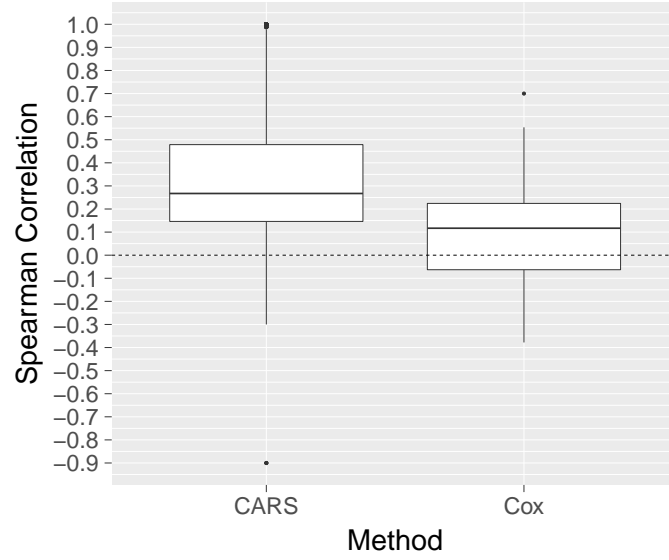


Fig. 6. Simulation study – scenario with high absolute correlations ($\rho = \pm 0.75$): The boxplots visualize the rank correlations of the estimated and the true covariate orderings, as obtained from variable selection by CARS scores, Cox scores and L_1 -penalized Cox regression. The censoring rate was equal to 25% and high absolute covariate correlations $\rho = \pm 0.75$. Each boxplot shows the results of 24300 simulation runs (3 explained variance ratios \times 3 signal to noise ratios \times 3 sample sizes \times 3 number of covariates \times 300 repetitions).

3.4 Scenario with high absolute correlations and high censoring rate

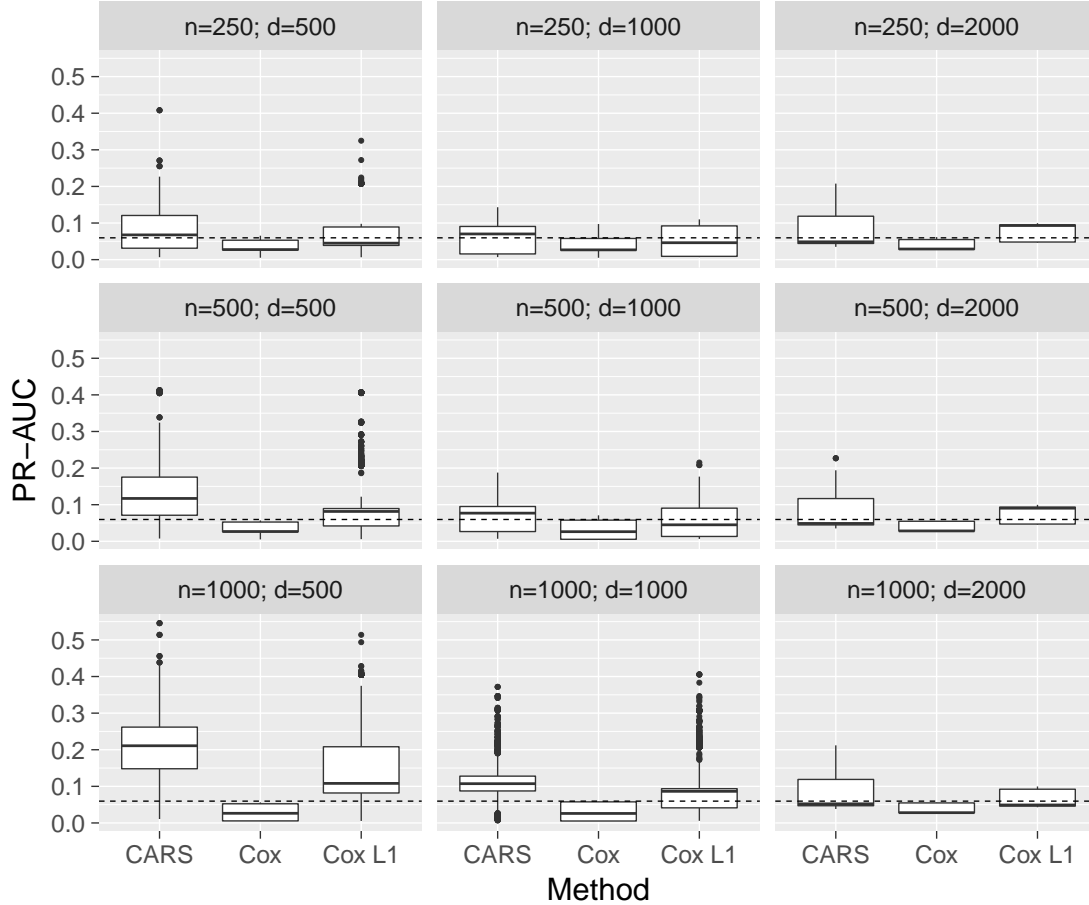


Fig. 7. Simulation: PR-AUC of all methods stratified by sample size (n) and number of covariates (d) with high absolute covariate correlations of $\rho = \pm 0.75$ and censoring rate of 75%. Each boxplot shows the results of 2700 simulation runs (3 explained variance ratios \times 3 signal to noise ratios \times 300 repetitions).

In this section the results of the scenario with high absolute correlations (third block of the correlation matrix, $\rho = \pm 0.75$) and with a high censoring rate of 75% are analyzed. This case is particularly challenging, as approximately 75% of the IPC weights become zero, implying that CARS scores were essentially computed from only 25% of the observations. Consider, for example, the cases $n \leq d$ in Figure 7, where the PR-AUC performance of all methods was nearly random. If sample size increased above the number of covariates $n > d$ the CARS score

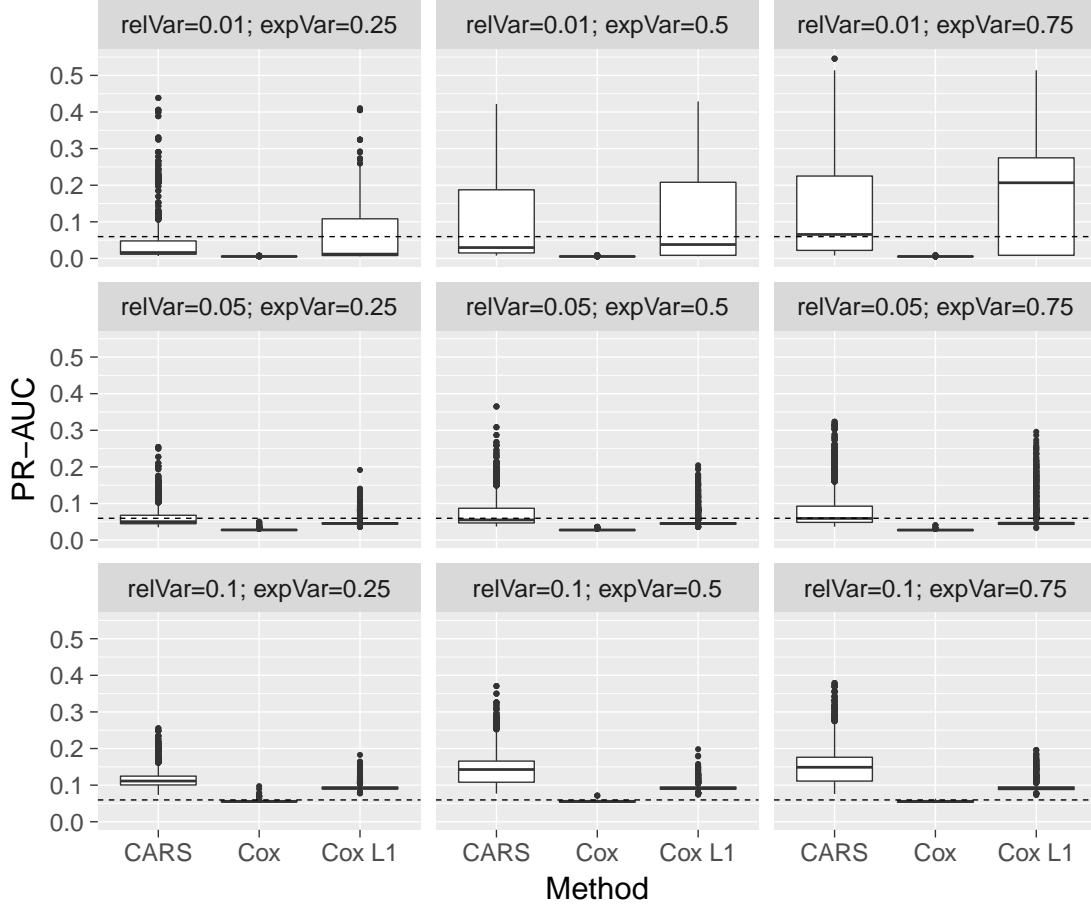


Fig. 8. Simulation: PR-AUC of CARS, Cox and Cox L_1 scores stratified by relative number of relevant variables (relVar) and explained variance (expVar) with high absolute covariate correlations of 0.75 and censoring rate of 25%. Each boxplot shows the results of 2700 simulation runs (3 sample sizes x 3 number of covariates x 300 repetitions).

median PR-AUC performance grew higher than the Cox approaches compared to the scenarios $n \leq d$. Increasing the number of influential covariates $\text{relVar} = 0.01$ to $\text{relVar} = 0.1$ yielded better CARS score PR-AUC performance. Especially in cases $\text{relVar} = 0.1$ and explained variance $\text{expVar} \geq 0.5$ CARS scores achieved better median results than Cox approaches. Regarding rank correlations both CARS and Cox approaches behaved similar as in the previous scenario with high correlations of $\rho = \pm 0.75$ and low censoring rate of 25% (Figure 9). The overall summaries with different correlation and censoring structures, averaged over all design parameters, are given

in the Appendix B.3. In the case with low censoring rates of 25% CARS scores performed better than Cox approaches. High censoring rates of 75% and high absolute covariate correlations of $\rho = \pm 0.75$ CARS scores and Cox scores with L_1 penalty were competitive, but without penalty Cox scores were below the PR-AUC of a random classifier.

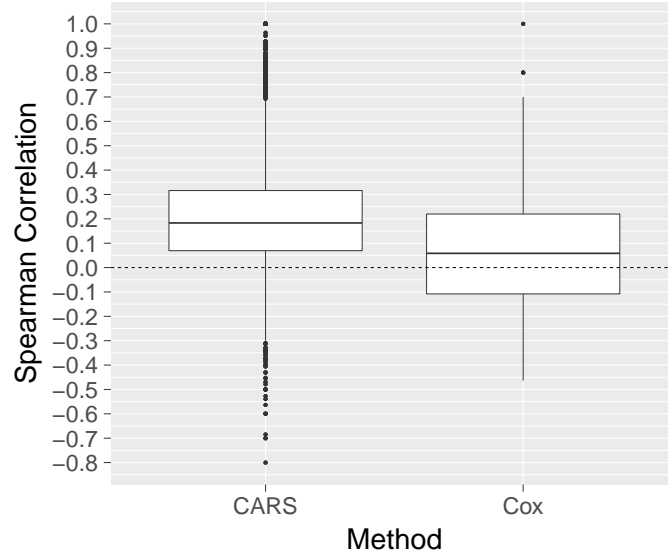


Fig. 9. Simulation study – scenario with high absolute correlations ($\rho = \pm 0.75$) and a high censoring rate of 75%: The boxplots visualize the rank correlations of the estimated and the true covariate orderings, as obtained from variable selection by CARS and Cox scores. Each boxplot shows the results of 24300 simulation runs (3 explained variance ratios x 3 signal to noise ratios x 3 sample sizes x 3 number of covariates x 300 repetitions).

3.5 Runtime in the low correlation, low censoring scenario

Besides the predictive performance the computational efficiency of the statistical methods is relevant in the analysis of high-dimensional genomic data. Therefore we additionally measured the computation of CARS, Cox and Cox L_1 scores without threshold models in the baseline scenario with low covariate correlations $\rho = \pm 0.25$ and low censoring rate 0.25. All run times were recorded without parallelization on the same computer with a processor Intel(R) Core(TM) i7-7700 CPU @ 4.20 Ghz and 16 GB RAM in *R* statistical software. CARS scores were computed by using *R* package *carSurv*. Cox scores were calculated by *R* packages *survival* and *glmnet*. Figure 10 shows that CARS scores are on average faster to compute than Cox scores with or without L_1 penalty for scenarios $n < 1000$. Especially in high dimensional context with low number of observations the magnitude between the run times of CARS compared to Cox approaches was large. In scenario $n = 1000, d = 500$ CARS and Cox approaches yielded comparable runtimes and in the cases $n = 1000, d > 500$ Cox approaches performed faster.

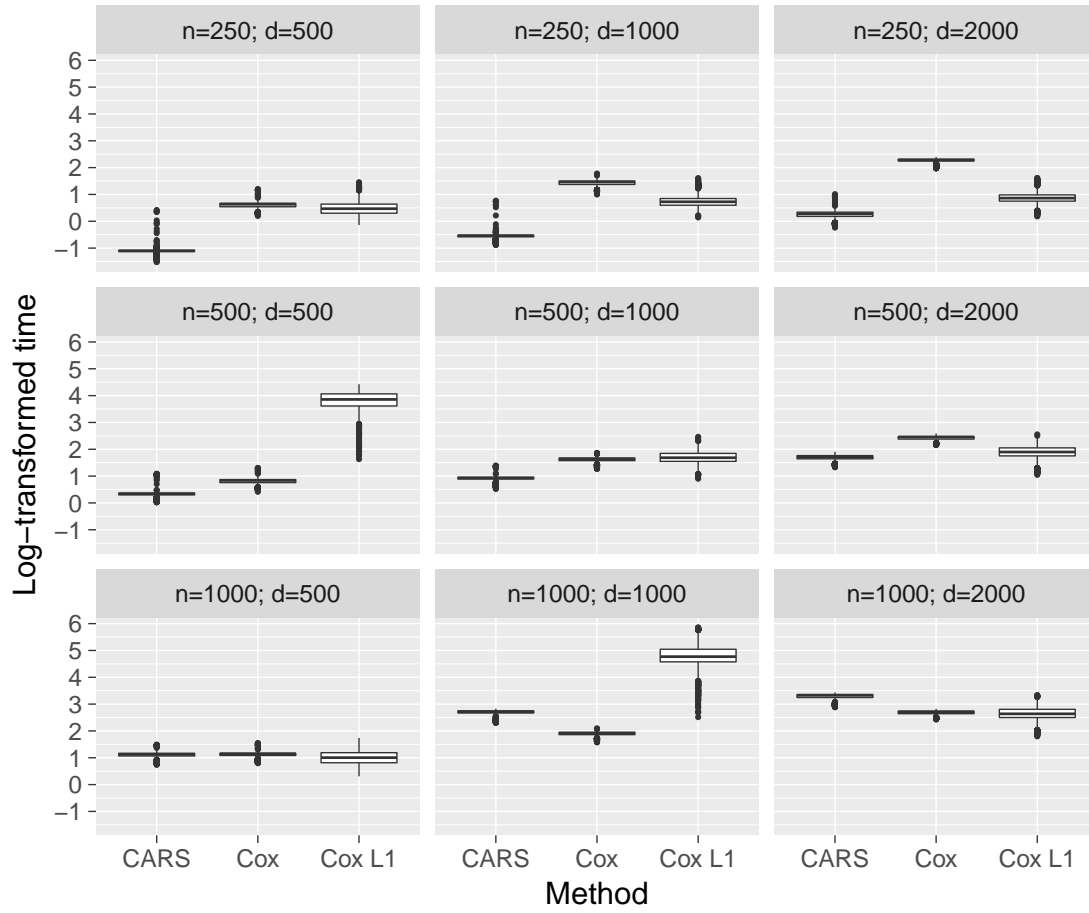


Fig. 10. Computational efficiency: Log-transformed time of the three methods CARS, Cox scores and Cox L_1 variable selection. The original time was measured in seconds without parallelization. Each boxplot shows the results of 2700 simulation runs (3 explained variance ratios \times 3 signal to noise ratios \times 300 repetitions).

3.6 Application to the Swedish Watchful Waiting Cohort

To investigate the properties of the proposed screening method in a real-world setting, we applied the CARS score to the Swedish Watchful Waiting Cohort data (Sboner *and others*, 2010). The data consists of 281 patients and 6157 variables. Beside the clinical covariates (such as patient age, Gleason score and year of diagnosis) an array of 6100 gene expression profiles (6K DASL) was designed by using four complementary DNA (cDNA)-mediated annealing, selection, ligation, and extension (DASL) assay panels (DAPs) (Fan *and others*, 2004; Bibikova *and others*, 2004). Further details of this procedure are available at GeneExpression Omnibus (GEO: <http://www.ncbi.nlm.nih.gov/geo/>) with platform accession number *GPL5474*. The data is also available at the GEO website with accession number *GSE16560*.

The study population included men who died from prostate cancer during follow up or survived at least 10 years after their diagnosis. The sample size was further restricted to men with high-density tumor regions and who did not receive any type of androgen deprivation. The event of interest was death of prostate cancer; 26.69% of the patients were censored. The median observed time was 100 months (range [6, 274] months). The median age was 74 years (range [51, 91] years), the median Gleason score was seven (range [2, 10]), and 58.72% of patients had a lethal diagnosis. The 2.5% and 97.5% quantiles of the Pearson correlations between the gene expressions were $[-0.2634, 0.2865]$ and the maximum absolute correlation was 0.9861. Therefore most genes were similar to the low correlation used in the simulation design (Section 3.1), in which CARS scores yielded favorable PR-AUC results. We applied CARS scores to screen for genes that influenced time to death of patients and evaluated their performance in comparison to Cox scores.

As the true effects of the genetic markers were unknown, it was not possible to analyze CARS and Cox scores by using the PR-AUC and rank correlation techniques considered in the previous

subsections. Instead, we evaluated the scores by comparing their ten times repeated ten-fold cross-validated predictive performance. The latter was measured by the time-dependent PR-AUC (Yuan *and others*, 2016), which is an extension of PR-AUC to censored data by applying inverse probability weighting (Van der Laan and Robins, 2003). The time-dependent PR-AUC can be interpreted as average positive predictive value. In addition, we computed a time-independent summary performance measure by weighting and integrating PR-AUC over time ("time-integrated PR-AUC", see Equation A.10 in Appendix A). In each of the 10×10 training folds CARS and Cox scores were estimated. Each set of risk score values was split into influential and non-influential genetic markers with a predefined q-value cut-off threshold $\alpha_1 \in \{0.01, 0.05, 0.1\}$. The cut-off threshold was compared to the q-values given by the method of Strimmer (2008) described in Section 2. For the Cox scores we used the same threshold procedure as CARS scores. All genetic markers with lower q-values than the specified threshold were selected and incorporated into a multivariable Cox regression model. Afterwards, the selected genetic markers were incorporated in a multivariable Cox regression model that also included a clinical baseline formula with the variables age, Gleason score and extremity diagnosis (patient group lethal or indolent) (Sboner *and others*, 2010). The performance of a random classifier corresponds to the time integrated event rate, which was calculated as the time-dependent event rate $P(T < t_0)$ averaged over all available time points t_0 within one fold. The average of the time integrated event rates was computed over 10×10 cross validation folds.

Time integrated PR-AUCs for each fold are shown in Figure 11. All methods had higher integrated PR-AUC than a random classifier across all cross validation folds. CARS score genetic marker selection resulted in similar predictive performance compared to genetic marker selection by Cox scores. Both approaches were fairly robust against the choice of the threshold α_1 . According to Figure 11, there appears to be no predictive benefit when genetic markers are added

to the clinical baseline formula, with CARS scores and Cox scores producing consistent results. This agrees with the findings in the original publication by Sboner *and others* (2010).

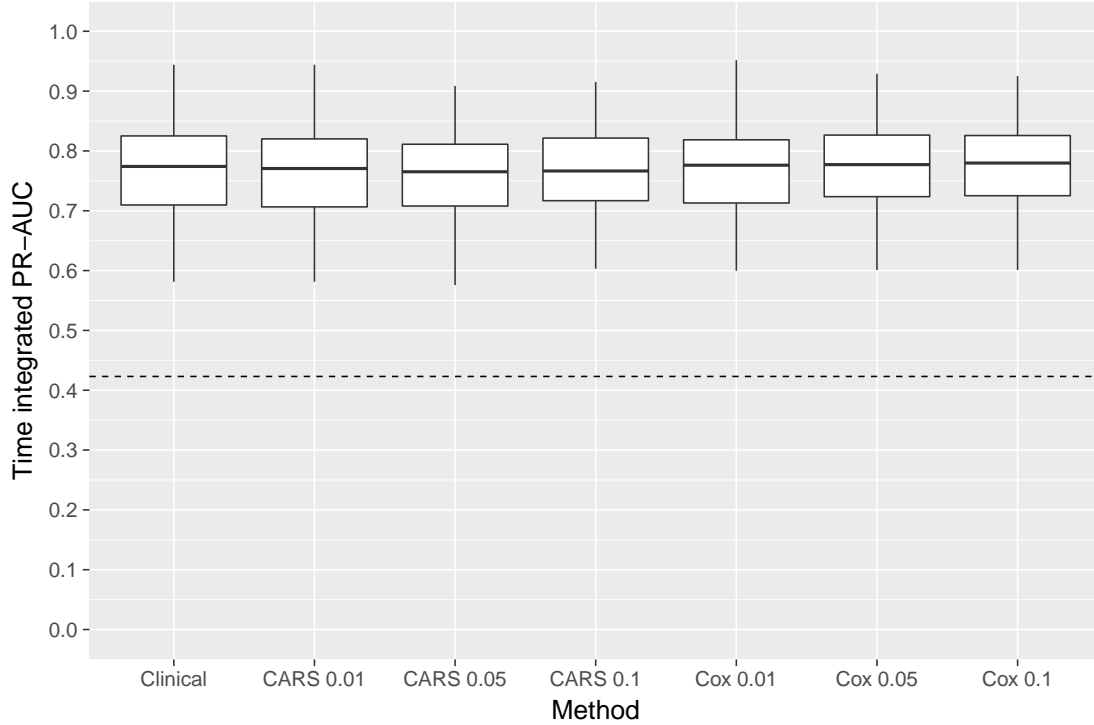


Fig. 11. Analysis of the Swedish Watchful Waiting Cohort: The boxplots show the integrated PR-AUCs of Cox models, as obtained from ten times repeated ten-fold cross-validation. In addition to the clinical baseline formula by Sboner *and others* (2010), the models contained genetic markers that were selected by CARS and Cox scores. The values $\{0.01, 0.05, 0.1\}$ represent different q-values cut-off thresholds. The dashed line denotes the average time integrated event rate and corresponds to the performance of a random classifier.

The complete data analysis with univariate CARS score screening resulted in 0, 3, and 10 identified genetic markers at the q-value thresholds $\alpha_1 = \{0.01, 0.05, 0.1\}$, respectively (see appendix Table C.1). Genetic marker selection by Cox scores yielded 1, 1 and 2 genetic markers at the same thresholds. Some of the selected genes by CARS scores with $\alpha_1 = 0.1$ match previous results from the literature: According to the NCBI database (NCBI, 2017), the BIRC5 baculoviral IAP repeat containing 5 is an inhibitor of apoptosis and found in most tumor cells. The gene

BMX non-receptor tyrosine kinase regulates differentiation and tumorigenicity of several types of cancer cells, and another gene (MLLT11, transcription factor 7 cofactor) was expressed in several leukemic cell lines. The complete list of identified genes with CARS scores is available in the appendix (Table C.1).

3.7 *Application to breast cancer microarray data*

In our second real-world example we applied CARS and Cox scores to an invasive breast cancer data set collected by Hatzis *and others* (2011); Itoh *and others* (2014). Merging both available microarray gene expression data sets in the NCBI database (Edgar *and others*, 2002, GEO accession numbers *GSE25055*, *GSE25065* and series *GSE25066*) resulted in 502 observations and 22338 variables. These can be partitioned into 55 clinical variables, metadata variables and 22283 gene expression markers. The data was collected using *GPL96* [HG-U133A] Affymetrix Human Genome U133A Arrays. The outcome was the time to distant relapse-free survival before surgery (median = 2.716 years, range = [0, 7.439] years. 21.91% of the patients had a relapse within the study duration. The 2.5% and 97.5% quantiles of the Pearson correlations between the gene expressions were $[-0.2467, 0.2725]$ and the maximum absolute correlation was 0.9986.

Analogous to the previous subsection, we used ten times repeated ten-fold cross-validation to analyze predictive performance. The clinical baseline model included the covariates age, tumor stage and an indicator of estrogen receptor (ER) positiveness. The genetic markers were selected by either CARS or Cox scores with different q-value thresholds $\alpha_1 = \{0.01, 0.05, 0.1\}$. The significant genetic markers were added to the clinical covariates, and a Cox regression model was fitted. Due to the large number of covariates, Cox regression was regularized with an L_1 penalty. The regularization parameter was tuned by internal 10-fold cross-validation as implemented in the *R* package *glmnet*.

The predictive performance of Cox regression based on CARS and Cox scores is shown in Figure 12. It is seen that CARS scores performed better than Cox scores for all levels of α_1 . For example, when using $\alpha_1 = 0.01$ as significance threshold, 22 out of the 22283 genetic markers were selected by the CARS-based procedure. Genetic marker selection based on Cox scores identified zero genetic markers at $\alpha_1 = 0.01$ and failed to include influential genetic markers, which degraded predictive performance. In contrast to the data Swedish Watchful Waiting Cohort, there were notable improvements in predictive performance when the genetic markers were added to the clinical model. All identified genes are presented in the appendix (Table C.1).

In order to annotate the 22 genes indicated by the CARS score as highly associated with survival at a q-value level $\alpha_1 < 0.01$ we conducted a gene set enrichment analysis based on gene ontology (GO) (Consortium, 2001) terms as implemented in the Bioconductor (Huber *and others*, 2015) package *topGO* (Alexa *and others*, 2006). The GO framework provides a set of structured vocabularies for specific biological domains that can be used to describe gene products in any organism. We computed Fisher’s test for enrichment of molecular function and report in supplementary Table C.2 the 32 GO terms that were enriched at p-value significance level $\alpha_2 < 0.05$. Among the five GO terms that had attained $\alpha_2 < 0.01$ in the Fisher enrichment test, we detected both protein-glycine ligase activity and protein-glycine ligase activity inhibition. Glycine metabolism has been associated with cancer cell proliferation (Amelio *and others*, 2014), and glycine uptake and catabolism can promote tumourigenesis and malignancy (Jain *and others*, 2012). The third enriched GO term was Ras guanyl-nucleotide exchange factor activity. Guanyl-nucleotide exchange factors are proteins that activate GTPases, which are enzymes binding and hydrolyzing guanosine triphosphate. Ras is one of the key oncogenes; although Ras mutations are comparatively rare in breast cancer, the RasGAP (Ras GTPase Activating Proteins) gene

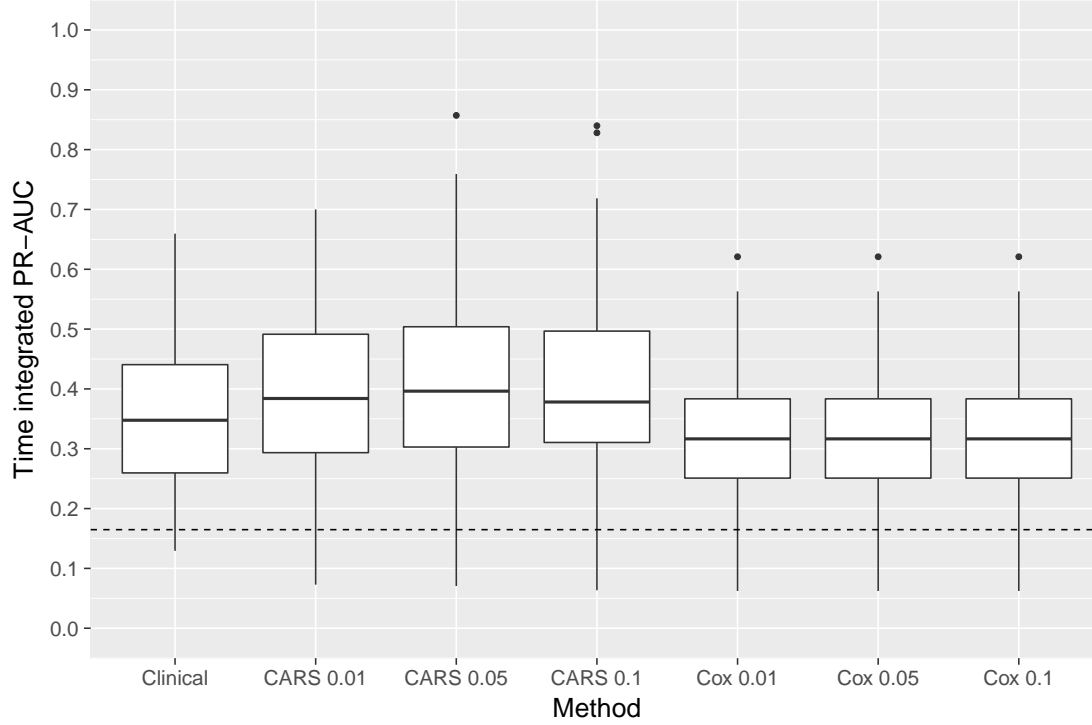


Fig. 12. Analysis of the breast cancer data by Hatzis *and others* (2011): The boxplots show the integrated PR-AUCs of L_1 -penalized Cox models, as obtained from ten-times repeated ten-fold cross-validation. In addition to the clinical baseline formula, the models contained genetic markers that were selected by CARS and Cox scores. The average time integrated event rate is displayed as a dashed line, which corresponds to the performance of a random classifier.

RASAL2 functions as tumour suppressor (McLaughlin *and others*, 2013). Furthermore we found enrichment evidence for sodium bicarbonate symporter activity, which enables the transfer of a solute or solutes from one side of a membrane to the other and has a central roles in pH regulation. Solid tumour exhibit different pH profiles compared to normal tissues, which points at a metabolic shift towards acid-producing pathways, reflecting both oncogenic signalling and the development of hypoxia (Gorbatenko *and others*, 2014). The sodium bicarbonate cotransporter NBCn1 is the predominant mechanism of acid extrusion in primary breast carcinomas compared to normal tissues (Boedtkjer *and others*, 2013) affecting intracellular pH levels. Finally we detected evidence of estrogen 16- α -hydroxylase activity, which is one of the earliest reported biomarkers for

breast cancer (Bradlow *and others*, 1986).

4. Summary and discussion

With high-dimensional omics data becoming more readily available in medical research, fast and efficient screening methods are needed for statistical model building and prediction. In this paper, we developed a framework for the selection of genetic markers in time-to-event models. This framework helps to improve biomarker discovery especially in high-dimensional settings with a large number of candidate variables. The proposed CARS score, which evaluates the associations between the de-correlated marker values and the time-to-event outcome, is estimated consistently by combining a set of IPC-weighted variance-covariance estimates. As shown in Section 2, estimates can be computed efficiently even when the number of candidate markers is large. Based on the rankings of the CARS score estimates, genetic markers can be selected for inclusion in a multivariable time-to-event model, where selection errors can be controlled by the adaptive false discovery rate density approach of Strimmer (2008).

In the numerical experiments presented in Section 3, CARS scores showed promising results with regard to the identification of influential marker variables. In particular, screening based on CARS scores outperformed traditional screening methods based on Cox scores in most of the analyzed scenarios. The proposed methodology resulted in increased PR-AUC values, and also in higher correlations between the rankings of the estimated and the true marker effects. With regard to predictive performance, the difference between CARS and Cox scores became largest when marker correlations were high. In these situations, the de-correlation of the markers – which is the key feature of CARS scores – had a particularly strong effect on the predictive performance of the multivariable models. Conversely, Cox-based screening – which ignores the correlations between markers – could not discriminate between noise and influential variables in low and high

covariate correlation settings, thereby degrading predictive performance. Since IPC-weighted estimators tend to have a high variance when censoring rates are high, we also evaluated the proposed estimators in scenarios with censoring rates as high as 75%. Even in these extreme cases, CARS-based screening did not result in a systematically worse performance than Cox-based screening. Furthermore the CARS scores are computationally efficient in high dimensional settings due to exploiting advanced matrix decompositions.

CARS scores are based on the theoretical framework of parametric accelerated failure time models. Future research could investigate how to extend this framework to semiparametric and/or nonlinear regression and different censoring mechanisms.

5. Software

All methods were implemented in *R* (R Core Team, 2017) and published as add-on package *carSurv* (Version 1.0.0), which is available from CRAN. Other packages used in this article include *survival* (Version 2.41-3) (Therneau, 2015), *fdrtool* (Version 1.2.15) (Klaus and Strimmer, 2015), *survAUC* (Version 1.0-5) (Potapov *and others*, 2012), *ggplot2* (Version 2.2.1) (Wickham, 2009), *mvnfast* (Fasiolo, 2016), *PRROC* (Version 1.3) (Grau *and others*, 2015) and *glmnet* (Version 2.0-13) (Simon *and others*, 2011).

Acknowledgements

Financial support from Deutsche Forschungsgemeinschaft (Project SCHM 2966/1-2) is gratefully acknowledged. Verena Zuber is supported by the Wellcome Trust and the Royal Society (Grant Number 204623/Z/16/Z) and the UK Medical Research Council (Grant Number MC_UU_00002/7). The authors thank Peter Welchowski for proof reading the manuscript.

APPENDIX

A. Proof of consistency of CAR survival scores

This section proves that the CAR survival score $\hat{\theta}$ is consistent for θ . CARS scores and their components are defined in the Equations A.1 to A.6. The proof is partitioned into four parts: Second the consistency of the weighted sample variance $s_{Y;w}^2$ of the response is evaluated in the next Section A.2. Third the consistency of the weighted response sample covariance $s_{X_j,Y;w}$ is analysed (Section A.3). In the last part the consistency of $\hat{\theta}$ is derived in Section A.4 by combining all previous parts together.

$$\hat{\theta} = \mathbf{R}_X^{-1/2} \mathbf{R}_{X,Y} \quad (\text{A.1})$$

$$\mathbf{R}_{X,Y} = \left(\frac{s_{X_j,Y;w}}{\sqrt{s_{X_j}^2} \sqrt{s_{Y;w}^2}} \right)_{j=1,\dots,d} \quad (\text{A.2})$$

$$s_{X_j,Y;w} = \frac{1}{n} \sum_{i=1}^n w_i (x_{ij} - \bar{x}_j) (\log(\tilde{t}_i) - \bar{y}_w) \quad (\text{A.3})$$

$$s_{X_j}^2 = \frac{1}{n-1} \sum_{i=1}^n (x_{i,j} - \bar{x}_j)^2 \quad (\text{A.4})$$

$$s_{Y;w}^2 = \frac{1}{n} \sum_{i=1}^n w_i (\log(\tilde{t}_i) - \bar{y}_w)^2 \quad (\text{A.5})$$

$$\bar{y}_w = \frac{1}{n} \sum_{i=1}^n w_i \log(\tilde{t}_i) \quad (\text{A.6})$$

A.1 Consistency of IPC weighted mean

To show the consistency of \bar{y}_w it is sufficient to embed this estimator into the framework of unbiased estimation equations (Huber, 1967). A weighted version of the unbiased estimation equations is used to account for censoring, which was developed in the context of nonresponse sample survey theory (Thompson, 1997; Skinner and Mason, 2012). In this context the unbiased estimating equation for parameter Θ is given by

$$\frac{1}{n} \sum_{i=1}^n \psi(\tilde{Y}_i, w_i, \Theta) = 0 \quad (\text{A.7})$$

$$E \left(\psi(\tilde{Y}_i, w_i, \Theta) \right) = 0 \quad \forall i = 1, \dots, n \quad (\text{A.8})$$

$$w_i = \frac{I(C_i \geq T_i)}{\hat{G}_n(\log(\tilde{T}_i))} \quad (\text{A.9})$$

$$\hat{G}_n(y) = \prod_{j: \log(\tilde{t}_i) \leq y} \left(1 - \frac{e_j}{r_j} \right) \quad (\text{A.10})$$

Under some regularity conditions given in Huber (1967) (e. g. measurability, continuity and uniqueness of solutions) the estimator of $\hat{\Theta}$ is consistent for Θ if Equation A.8 holds. The weights w_i are inverse probability censoring adjustments based on the ideas of the Horvitz Thompson estimator (Horvitz and Thompson, 1952). Each observation $i = 1, \dots, n$ of the data contains the observed time response, event indicator and covariates $(y_i = \log(\tilde{t}_i), \Delta_i, \mathbf{x}_i)$. The estimate of the logarithmic censoring survivor function $\hat{G}_n(\log(t))$ corresponds to the Kaplan-Meier product estimator (Kaplan and Meier, 1958) with individuals at risk r_j just prior the actual $\log(t)$ and number of observed events e_j . The Kaplan-Meier product estimator is consistent and therefore the empirical estimate can be replaced by the true survival function in asymptotic analysis. From now on assume that $G(y)$ is known, $G(y) > \nu > 0$ with a small real number ν , $T_i > 0$; $C_i > 0$ and independence of survival and censoring times. Next consider the estimation equation for the weighted mean \bar{y}_w :

$$\psi(\tilde{Y}_i, w_i, \mu_{\log(T)}) = w_i \log(\tilde{t}_i) - \mu_{\log(T)} \quad (\text{A.11})$$

$$E(w_i \log(\tilde{t}_i)) = \int_{-\infty}^{\infty} \int_{-\infty}^{\infty} \frac{I(\log(C_i) \geq \log(T_i))}{G(\log(\tilde{T}_i))} \log(\tilde{T}_i) f_{\log(T)}(\log(T)) f_{\log(C)}(\log(C)) d\log(T) d\log(C) \quad (\text{A.12})$$

The indicator function $I(\log(C_i) \geq \log(T_i))$ states that only observed survival times contribute to $\psi(\tilde{Y}_i, w_i, \mu_T)$ and therefore \tilde{T}_i can be replaced by T_i . The next steps following Equation

A.13 show that \bar{y}_w is unbiased for the parameter $\mu_{\log(T)}$. It follows under regularity conditions that \bar{y}_w is a consistent estimator of $\mu_{\log(T)}$:

$$E(w_i \log(\tilde{t}_i)) = \int_{-\infty}^{\infty} \frac{1}{G(\log(T_i))} \log(T_i) f_{\log(T)}(\log(T))$$

$$\int_{\log(t_i)}^{\infty} f_{\log(C)}(\log(C)) d\log(T) d\log(C) \quad (\text{A.13})$$

$$= \int_{-\infty}^{\infty} \frac{G(\log(T_i))}{G(\log(T_i))} \log(T_i) f_{\log(T)}(\log(T)) d\log(T) \quad (\text{A.14})$$

$$= \mu_{\log(T)} \quad (\text{A.15})$$

A.2 Consistency of IPC weighted variance

The unbiasedness of \bar{y}_w with respect to $\mu_{\log(T)}$ allows to replace \bar{y}_w in the weighted variance estimator $s_{Y;w}^2$ by the true value $\mu_{\log(T)}$ in asymptotic analysis. The ψ transformation for the weighted variance estimator $s_{Y;w}^2$ is given by

$$\psi(\tilde{Y}_i, w_i, \sigma_{\log(T)}^2) = w_i (\log(T_i) - \mu_{\log(T)})^2 - \sigma_{\log(T)}^2 \quad (\text{A.16})$$

$$= w_i \log(T_i)^2 - 2w_i \log(T_i) \mu_{\log(T)} + w_i \mu_{\log(T)}^2 - \sigma_{\log(T)}^2 \quad (\text{A.17})$$

The expectation of the weights w_i equal one and therefore the two middle terms of Equation A.17 cancel each other out:

$$E(w_i) = \int_{-\infty}^{\infty} \int_{-\infty}^{\infty} \frac{I(\log(C_i) \geq \log(T_i))}{G(\log(\tilde{T}_i))} f_{\log(T)}(\log(T)) f_{\log(C)}(\log(C)) d\log(T) d\log(C) \quad (\text{A.18})$$

$$= \int_{-\infty}^{\infty} \frac{1}{G(\log(\tilde{T}_i))} f_{\log(T)}(\log(T)) \int_{\log(t_i)}^{\infty} f_{\log(C)}(\log(C)) d\log(T) d\log(C) \quad (\text{A.19})$$

$$= \int_0^{\infty} \frac{G(\log(\tilde{T}_i))}{G(\log(\tilde{T}_i))} f_{\log(T)}(\log(T)) d\log(T) = 1 \quad (\text{A.20})$$

$$\Rightarrow E\left(w_i (\log(\tilde{T}_i) - \mu_{\log(T)})^2\right) = E(w_i \log(\tilde{T}_i)^2) - \mu_{\log(T)}^2 \quad (\text{A.21})$$

The remaining stochastic term $w_i \log(\tilde{T}_i)^2$ is further evaluated. Using the same reasoning as in Section A.1 the expectation yields unbiasedness of the estimating equation $\frac{1}{n} \sum_{i=1}^n \psi(\tilde{Y}_i, w_i, \sigma_{\log(T)}^2)$ for $\sigma_{\log(T)}^2$ (see Equations A.22 to A.26). Therefore the estimator $s_{Y;w}^2$ is consistent for $\sigma_{\log(T)}^2$.

$$E(w_i \log(\tilde{T}_i)^2) = \int_{-\infty}^{\infty} \int_{-\infty}^{\infty} \frac{I(\log(C_i) \geq \log(\tilde{T}_i))}{G(\log(\tilde{T}_i))} \log(\tilde{T}_i)^2 f_{\log(T)}(\log(T)) f_{\log(C)}(\log(C)) d\log(T) d\log(C) \quad (\text{A.22})$$

$$= \int_{-\infty}^{\infty} \frac{1}{G(\log(\tilde{T}_i))} \log(\tilde{T}_i)^2 f_{\log(T)}(\log(T)) \int_{\log(t_i)}^{\infty} f_{\log(C)}(\log(C)) d\log(T) d\log(C) \quad (\text{A.23})$$

$$= \int_{-\infty}^{\infty} \log(\tilde{T}_i)^2 f_{\log(T)}(\log(T)) d\log(T) \quad (\text{A.24})$$

$$= \sigma_{\log(T)}^2 + \mu_{\log(T)}^2 \quad (\text{A.25})$$

$$\Rightarrow E\left(\psi(\tilde{Y}_i, w_i, \sigma_{\log(T)}^2)\right) = 0 \quad (\text{A.26})$$

A.3 Consistency of IPC weighted covariance

Following the same strategy as in the previous Section A.2 the estimating equation is adapted to the sample covariance estimator $s_{X_j, Y; w}$:

$$\psi\left(\tilde{Y}_i, w_i, \sigma_{X_j, \log(T)}\right) = w_i(x_{ij} - \mu_j) (\log(\tilde{t}_i) - \mu_{\log(T)}) - \sigma_{X_j, \log(T)} \quad (\text{A.27})$$

$$= \underbrace{w_i x_{ij} \log(\tilde{t}_i)}_F - \underbrace{w_i x_{ij} \mu_{\log(T)}}_G - \underbrace{w_i \mu_j \log(\tilde{t}_i)}_H + w_i \mu_j \mu_{\log(T)} - \sigma_{X_j, \log(T)} \quad (\text{A.28})$$

The order of multiple Riemann integrals can be switched without changing the final result (Elstrodt, 2011). The analysis of the expectations F, G, H yields

$$E(F) = \int_{-\infty}^{\infty} \int_{-\infty}^{\infty} \int_{-\infty}^{\infty} \frac{I(\log(C_i) \geq \log(T_i))}{G(\log(\tilde{T}_i))} \log(\tilde{T}_i) X_{i,j} f_{\log(T), X_j}(\log(T), X_j) f_{\log(C)}(\log(C)) d\log(T) dX_j d\log(C) \quad (\text{A.29})$$

$$= \int_{-\infty}^{\infty} \int_{-\infty}^{\infty} \log(T_i) X_{i,j} f_{\log(T), X_j}(\log(T), X_j) d\log(T) dX_j = \sigma_{X_j, \log(T)} + \mu_j \mu_{\log(T)} \quad (\text{A.30})$$

$$E(G) = \mu_{\log(T)} \int_{-\infty}^{\infty} \int_{-\infty}^{\infty} \int_{-\infty}^{\infty} \frac{I(\log(C_i) \geq \log(T_i))}{G(\log(\tilde{T}_i))} X_{i,j} f_{X_j, \log(T)}(X_j, \log(T)) f_{\log(C)}(\log(C)) dX_j d\log(T) d\log(C) \quad (\text{A.31})$$

$$= \mu_{\log(T)} \int_{-\infty}^{\infty} X_j \int_{-\infty}^{\infty} f_{X_j, \log(T)}(X_j, \log(T)) dX_j d\log(T) \quad (\text{A.32})$$

$$= \mu_{\log(T)} \int_{-\infty}^{\infty} X_j f_{X_j}(X_j) dX_j = \mu_j \mu_{\log(T)} \quad (\text{A.33})$$

$$E(H) = \mu_j \int_{-\infty}^{\infty} \int_{-\infty}^{\infty} \frac{I(\log(C_i) \geq \log(T_i))}{G(\log(\tilde{T}_i))} \log(\tilde{T}_i) f_{\log(T)}(\log(T)) f_{\log(C)}(\log(C)) d\log(T) d\log(C) \quad (\text{A.34})$$

$$= \mu_j \int_{-\infty}^{\infty} \log(T_i) f_{\log(T)}(\log(T)) d\log(T) = \mu_j \mu_{\log(T)} \quad (\text{A.35})$$

Combining the results F, G, H with the other terms of the Equation A.28 shows the unbiasedness of $\psi\left(\tilde{Y}_i, w_i, \sigma_{X_j, \log(T)}\right)$ for the parameter $\sigma_{X_j, \log(T)}$. The consistency follows from the theory of unbiased estimating equations (Huber, 1967):

$$E(G) = E(H) \quad (\text{A.36})$$

$$E\left(\psi\left(\tilde{Y}_i, w_i, \sigma_{X_j, \log(T)}\right)\right) = E(F) - E(G) - E(H) + \mu_j \mu_{\log(T)} - \sigma_{X_j, \log(T)} \quad (\text{A.37})$$

$$= 0 \quad (\text{A.38})$$

A.4 *Combination of proof results*

In this section all previous consistency proofs of weighted mean, weighted variance and weighted covariance are combined together to the CARS score. If $\mathbf{P}_{\mathbf{X}, Y}$ are the true pairwise correlations between the covariates and the response, it follows that

$$\lim_{n \rightarrow \infty} \mathbf{R}_{\mathbf{X}, Y} = \lim_{n \rightarrow \infty} \left(\frac{s_{Y, X_j; w}}{s_{X_j} s_{Y; w}} \right)_{j=1, \dots, d} \longrightarrow \mathbf{P}_{\mathbf{X}, Y} \quad (\text{A.39})$$

is consistent too, because product and quotient transformations of three consistent estimators are likewise consistent (Lehmann, 1998). Another part of the CARS score is the shrinkage estimator $\mathbf{R}_{\text{Shrink}}$ of the correlations between the covariates $\mathbf{R}_{\mathbf{X}}$ (Schäfer and Strimmer, 2005)

$$\mathbf{R}_{\text{Shrink}} = \lambda \mathbf{I}_p + (1 - \lambda) \mathbf{R}_{\mathbf{X}} \quad (\text{A.40})$$

$$\hat{\lambda} = \frac{\sum_{j \neq k} \widehat{\text{Var}}(\hat{r}_{j,k})}{\sum_{j \neq k} \hat{r}_{j,k}^2} \quad (\text{A.41})$$

$$\hat{r}_{j,k} = \frac{\frac{1}{n-1} \sum_{i=1}^n (x_{i,j} - \bar{x}_j)(x_{i,k} - \bar{x}_k)}{\sqrt{\frac{1}{n-1} \sum_{i=1}^n (x_{i,j} - \bar{x}_j)^2} \sqrt{\frac{1}{n-1} \sum_{i=1}^n (x_{i,k} - \bar{x}_k)^2}} \quad (\text{A.42})$$

The shrinkage parameter λ is estimated as well. $\mathbf{I}_p \in \mathbb{Z}^{p \times p}$ is the unit matrix. $\hat{r}_{j,k}$ are the sample correlations between the j -th and k -th variables. In the limit the estimator converges to zero:

$$\lim_{n \rightarrow \infty} \hat{\lambda} = \frac{\lim_{n \rightarrow \infty} \sum_{j \neq k} \widehat{Var}(\hat{r}_{j,k})}{\lim_{n \rightarrow \infty} \sum_{j \neq k} \hat{r}_{j,k}^2} \quad (\text{A.43})$$

$$= \frac{\sum_{j \neq k} \lim_{n \rightarrow \infty} \widehat{Var}(\hat{r}_{j,k})}{\sum_{j \neq k} \lim_{n \rightarrow \infty} \hat{r}_{j,k}^2} \quad (\text{A.44})$$

$$= \frac{\sum_{j \neq k} 0}{\sum_{j \neq k} r_{j,k}^2} = 0 \quad (\text{A.45})$$

$$\Rightarrow \lim_{n \rightarrow \infty} \hat{\lambda} = 0 \quad (\text{A.46})$$

Because $\hat{r}_{j,k}$ is a consistent estimator of $r_{j,k}$, the variance of this estimator $\widehat{Var}(\hat{r}_{j,k})$ must converge to zero. Subsequent the shrinkage parameter converges to zero. If $\lambda = 0$, then $\mathbf{R}_{\text{Shrink}} = \mathbf{R}_{\mathbf{X}}$ which is itself a consistent estimator of the covariates correlation matrix $\mathbf{P}_{\mathbf{X}}$. Further the inverse square root $\mathbf{R}_{\text{shrink}}^{-1/2}$ of the shrinkage estimator is consistent too, because the transformation function is continuous. Combining all previous results shows the consistency of CARS $\hat{\boldsymbol{\theta}} = \mathbf{R}_{\text{shrink}}^{-1/2} \mathbf{R}_{\mathbf{X},Y}$ for $\boldsymbol{\theta}$, because it is a product of two consistent estimators.

B. Additional results obtained from the simulation study

B.1 *CARS simulation with low absolute covariate correlations*

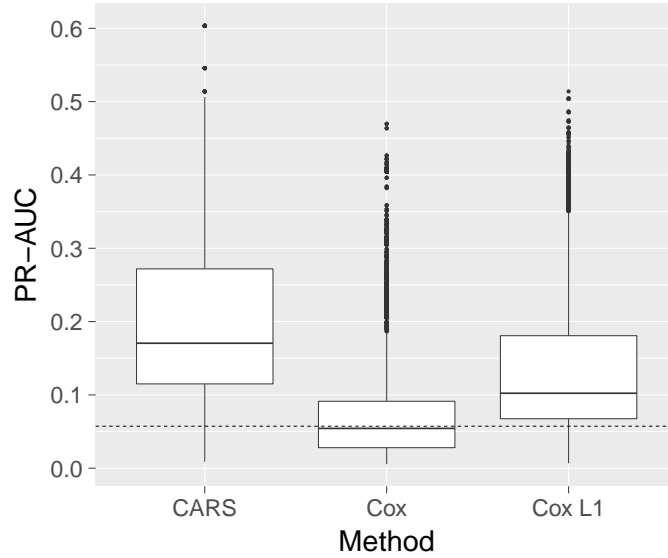


Fig. 13. Simulation study – scenario with low absolute correlations ($\rho = \pm 0.25$): The boxplots visualize the PR-AUC values obtained from variable selection by CARS scores, Cox scores and L_1 -penalized Cox regression. The censoring rate was equal to 0.25. The average prevalence of the positive class (computed from all simulations) is displayed by a dashed line. Note that the boxplots contain the PR-AUC values corresponding to all three rates of influential covariates (1%, 5%, 10%). Each boxplot shows the results of 24300 simulation runs (3 explained variance ratios x 3 signal to noise ratios x 3 sample sizes x 3 number of covariates x 300 repetitions).

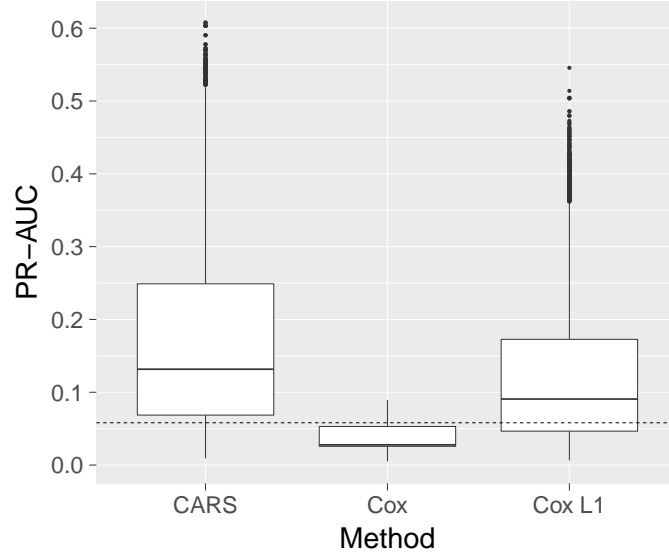
B.2 *CARS simulation with high absolute covariate correlations*

Fig. 14. Simulation study – scenario with high absolute correlations ($\rho = \pm 0.75$): The boxplots visualize the PR-AUC values obtained from variable selection by CARS scores, Cox scores and L_1 -penalized Cox regression. The censoring rate was equal to 0.25. The average prevalence of the positive class (computed from all simulations) is displayed by a dashed line. Note that the boxplots contain the PR-AUC values corresponding to all three rates of influential covariates (1%, 5%, 10%). Each boxplot shows the results of 24300 simulation runs (3 explained variance ratios x 3 signal to noise ratios x 3 sample sizes x 3 number of covariates x 300 repetitions). Cox scores interquartile range is below PR-AUC of a random classifier.

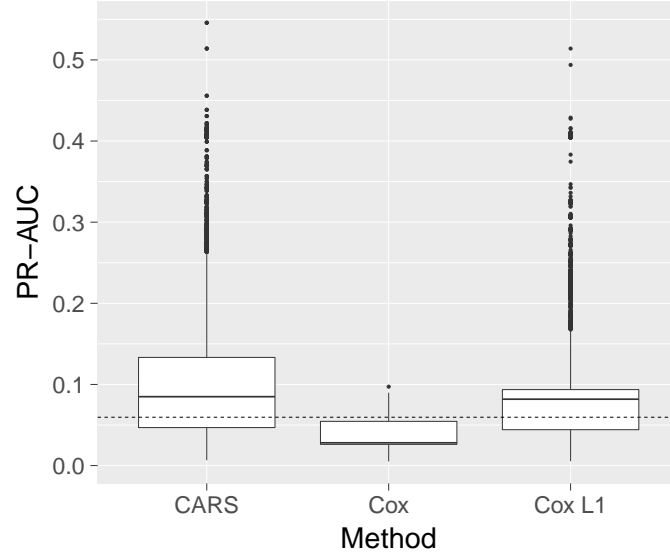
B.3 *CARS simulation with high absolute covariate correlations and censoring rate**0.75*

Fig. 15. Simulation study – scenario with high absolute correlations ($\rho = \pm 0.75$) and a high censoring rate of 0.75: The boxplots visualize the PR-AUC values obtained from variable selection by CARS scores, Cox scores and L_1 -penalized Cox regression. The average prevalence of the positive class (computed from all simulations) is displayed by a dashed line. Note that the boxplots contain the PR-AUC values corresponding to all three rates of influential covariates (1%, 5%, 10%). Each boxplot shows the results of 24300 simulation runs (3 explained variance ratios x 3 signal to noise ratios x 3 sample sizes x 3 number of covariates x 300 repetitions). Cox scores interquartile range is below PR-AUC of a random classifier.

B.4 Construction of correlation matrix

In this section give more details for the construction of the correlation matrices used in the simulation (see Section 3.1). First a preparatory design matrix \mathbf{A} is created. \mathbf{A} is partitioned in three blocks of equal size. The correlations between covariates cover a small range in the first block, medium range in the second block and a larger range in the third block. Within each block, half of all correlations are positive and the other half is negative. For example consider the case with 12 covariates: Then each design block would be given by the matrix

$$\mathbf{A} = \begin{pmatrix} 1 & \xi & \xi & -\xi \\ \xi & 1 & \xi & -\xi \\ \xi & \xi & 1 & -\xi \\ -\xi & -\xi & -\xi & 1 \end{pmatrix} \quad (\text{B.1})$$

with $\xi = \{0.25, 0.5, 0.75\}$ in the corresponding blocks. All correlations between variables belonging to different blocks are set to zero. Then the prepared matrix is converted to the nearest possible positive definite matrix \mathbf{B} , measured by a weighted Frobenius Norm $\|\mathbf{B}\|_W$ of the elementwise differences between the specified and new matrix:

$$\Omega(\mathbf{B}) = \min \{\|\mathbf{A} - \mathbf{B}\|_W : \mathbf{B} \text{ is a correlation matrix}\} \quad (\text{B.2})$$

$$\|\mathbf{B}\|_W = \|\mathbf{W} \circ \mathbf{B}\|_F; \quad \mathbf{W} \text{ symmetric and positive} \quad (\text{B.3})$$

$$\|\mathbf{B}\|_F^2 = \sum_{i,j} b_{i,j}^2 \quad (\text{B.4})$$

Here \circ denotes the Hadamard product (elementwise matrix multiplication) and $b_{i,j}$ are the elements of matrix \mathbf{B} . For further details of the algorithm to minimize the deviations $\Omega(\mathbf{B})$ from \mathbf{A} we refer to Higham (2002). A histogram with relative frequencies of the correlation matrix entries, after applying the algorithm, above the diagonal based on 1000 covariates are shown in the next figure:

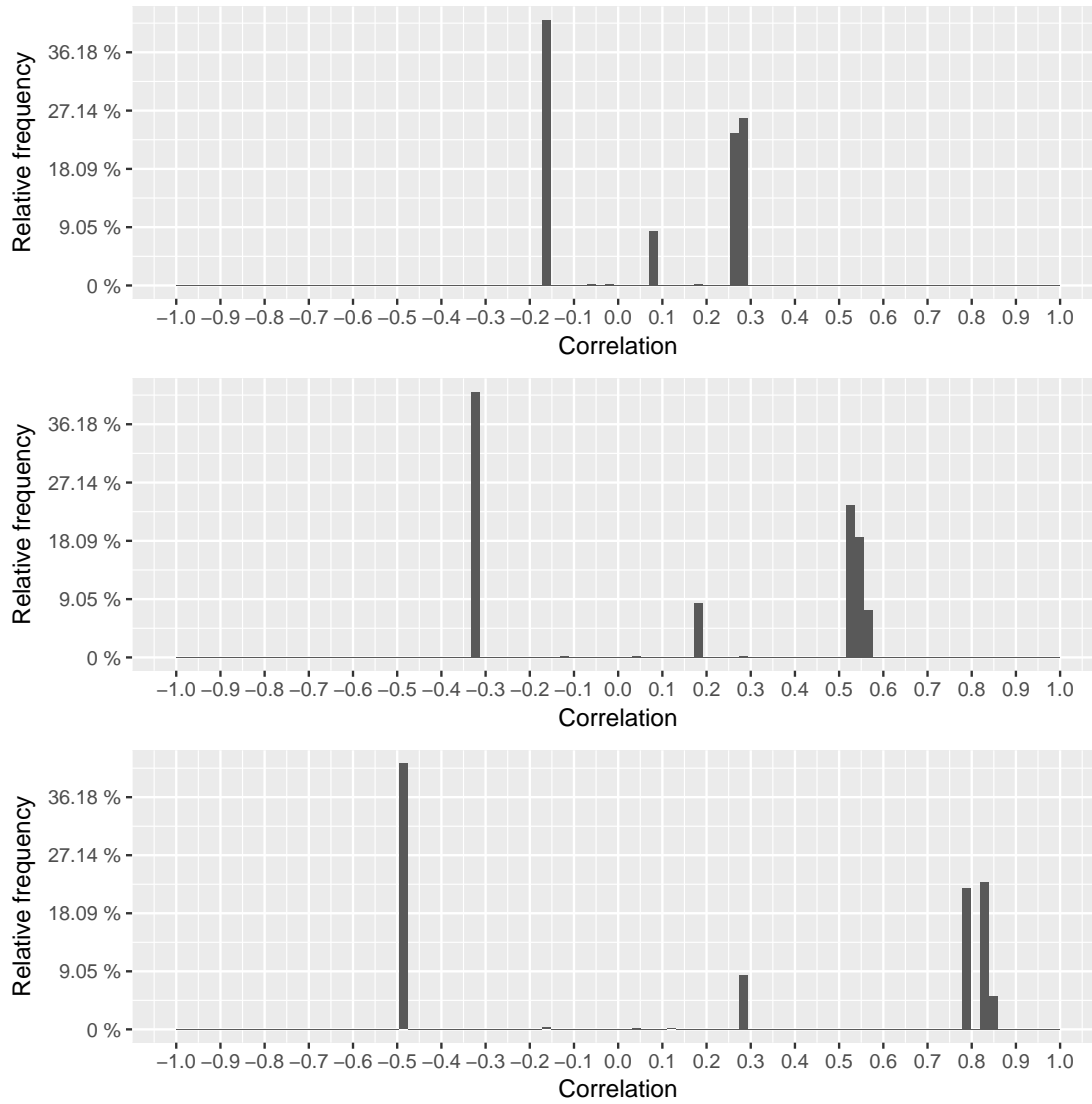


Fig. 16. The top figure shows the histogram (100 equal sized intervals) of the first block of the final correlation matrix with 1000 covariates. Only correlations above the diagonal are shown. Middle figure shows the histogram of the second block and the lower figure gives the relative frequencies of the third block.

C. Additional material used for the data analysis

C.1 *CARS scores: Selected variables in data analysis*

Gene symbol	CARS score	Q-value
NM_007244	0.1063	0.0461
NM_004912	-0.1035	0.0461
NM_203281	-0.1016	0.0461
NM_001012271	-0.0944	0.0814
NM_021992	-0.0939	0.0835
NM_006818	0.0939	0.0836
NM_005722	-0.0928	0.0877
NM_003855	-0.0923	0.0895
NM_001186	-0.0916	0.0918
NM_006846	0.0906	0.0965

Table 1. Prostate cancer: CARS scores and q-values below $\alpha = 0.1$ ordered by absolute score magnitude. Gene symbol refers to the accession number in the NCBI database (Edgar *and others*, 2002).

Gene Symbol	CARS score	Q-value
GRIN2C	-0.0479	$1.0560 * 10^{-6}$
RGP1	0.0446	$6.8075 * 10^{-6}$
TSPAN5	0.0446	$6.8776 * 10^{-6}$
RGS12	0.0441	$7.7700 * 10^{-6}$
ITGA2B	0.0404	$1.1334 * 10^{-4}$
SURF1	-0.0402	$1.3162 * 10^{-4}$
ZC2HC1A	0.0386	$3.7071 * 10^{-4}$
MCM9	0.0369	$1.0399 * 10^{-3}$
TRRAP	0.0368	$1.0732 * 10^{-3}$
SLC4A5	0.0360	$1.7160 * 10^{-3}$
FEZ2	-0.0356	$2.1184 * 10^{-3}$
ARPC4 /// ARPC4-TTLL3 /// TTLL3	0.0347	$3.2360 * 10^{-3}$
KERA	0.0347	$3.3192 * 10^{-3}$
GPR98	0.0341	$4.4523 * 10^{-3}$
SEPT6	0.0336	$5.6147 * 10^{-3}$
PRUNE2	0.0334	$6.1200 * 10^{-3}$
PLEKHG3	0.0332	$6.6953 * 10^{-3}$
AW973834 ¹	0.0329	$7.4615 * 10^{-3}$
CYP2C8	0.0326	$8.2900 * 10^{-3}$
CUZD1	0.0326	$8.4730 * 10^{-3}$
CTSF	0.0324	$8.8681 * 10^{-3}$
KIAA0485	0.0323	$9.0860 * 10^{-3}$

Table 2. Breast cancer: CARS scores and q-values below $\alpha = 0.01$ ordered by absolute score magnitude. Gene symbol refers to the accession number in the NCBI database (Edgar *and others*, 2002) or proteins.

C.2 *Summary of gene enrichment analysis*

GO.ID	Term	Ann	Signif	Expect	p-value
GO:0070735	Protein-glycine ligase activity	2	1	0	0.0020
GO:0070736	Protein-glycine ligase activity	2	1	0	0.0020
GO:0005088	Ras guanyl-nucleotide exchange factor	373	3	0.35	0.0057
GO:0008510	Sodium:bicarbonate symporter activity	10	1	0.01	0.0099
GO:0101020	Estrogen 16-alpha-hydroxylase activity	10	1	0.01	0.0099
GO:0005085	Guanyl-nucleotide exchange factor activity	470	3	0.44	0.0107
GO:0004972	NMDA glutamate receptor activity	13	1	0.01	0.0128
GO:0070051	Fibrinogen binding	13	1	0.01	0.0128
GO:0033695	Oxidoreductase activity acting on CH	15	1	0.01	0.0148
GO:0034875	Caffeine oxidase activity	15	1	0.01	0.0148
GO:0016881	Acid-amino acid ligase activity	21	1	0.02	0.0207
GO:0005452	Inorganic anion exchanger activity	22	1	0.02	0.0217
GO:0015106	Bicarbonate transmembrane transporter activity	23	1	0.02	0.0226
GO:0016725	Oxidoreductase activity, acting on CH	23	1	0.02	0.0226
GO:0015301	Anion:anion antiporter activity	26	1	0.02	0.0255
GO:0004970	Ionotropic glutamate receptor activity	29	1	0.03	0.0284
GO:0005234	Extracellular-glutamate-gated ion channel	30	1	0.03	0.0294
GO:0008324	Cation transmembrane transporter activity	703	3	0.66	0.0309
GO:0004129	Cytochrome-c oxidase activity	33	1	0.03	0.0323
GO:0015002	Heme-copper terminal oxidase activity	33	1	0.03	0.0323
GO:0016676	Oxidoreductase activity	33	1	0.03	0.0323
GO:0008391	Arachidonic acid monooxygenase activity	34	1	0.03	0.0333
GO:0008392	Arachidonic acid epoxygenase activity	34	1	0.03	0.0333
GO:0016675	Oxidoreductase activity	34	1	0.03	0.0333
GO:0070330	Aromatase activity	34	1	0.03	0.0333
GO:0017112	Rab guanyl-nucleotide exchange factor activity	39	1	0.04	0.0381
GO:0008066	Glutamate receptor activity	42	1	0.04	0.0409
GO:0016712	Oxidoreductase activity	42	1	0.04	0.0409
GO:0022824	Transmitter-gated ion channel activity	44	1	0.04	0.0429
GO:0022835	Transmitter-gated channel activity	44	1	0.04	0.0429
GO:0015296	Anion:cation symporter activity	46	1	0.04	0.0448
GO:0008395	Steroid hydroxylase activity	50	1	0.05	0.0486

Table 3. Breast cancer: Gene enrichment analysis based on Fisher's test with *R* package *topGO*. The first column gives the gene ontology (GO) (Consortium, 2001) identification number and column "Term" gives additional details. The number in column "Ann" shows how many genes are annotated with the GO term. Column "Signif" gives the number of significant genes of the GO term with respect to q-value 0.05. "Expect" shows the expected number of significant genes under the null hypothesis, e.g. no genes are enriched. The last column "p-value" gives the p-value for Fisher's test for enrichment.

C.3 CARS scores diagnostic plots

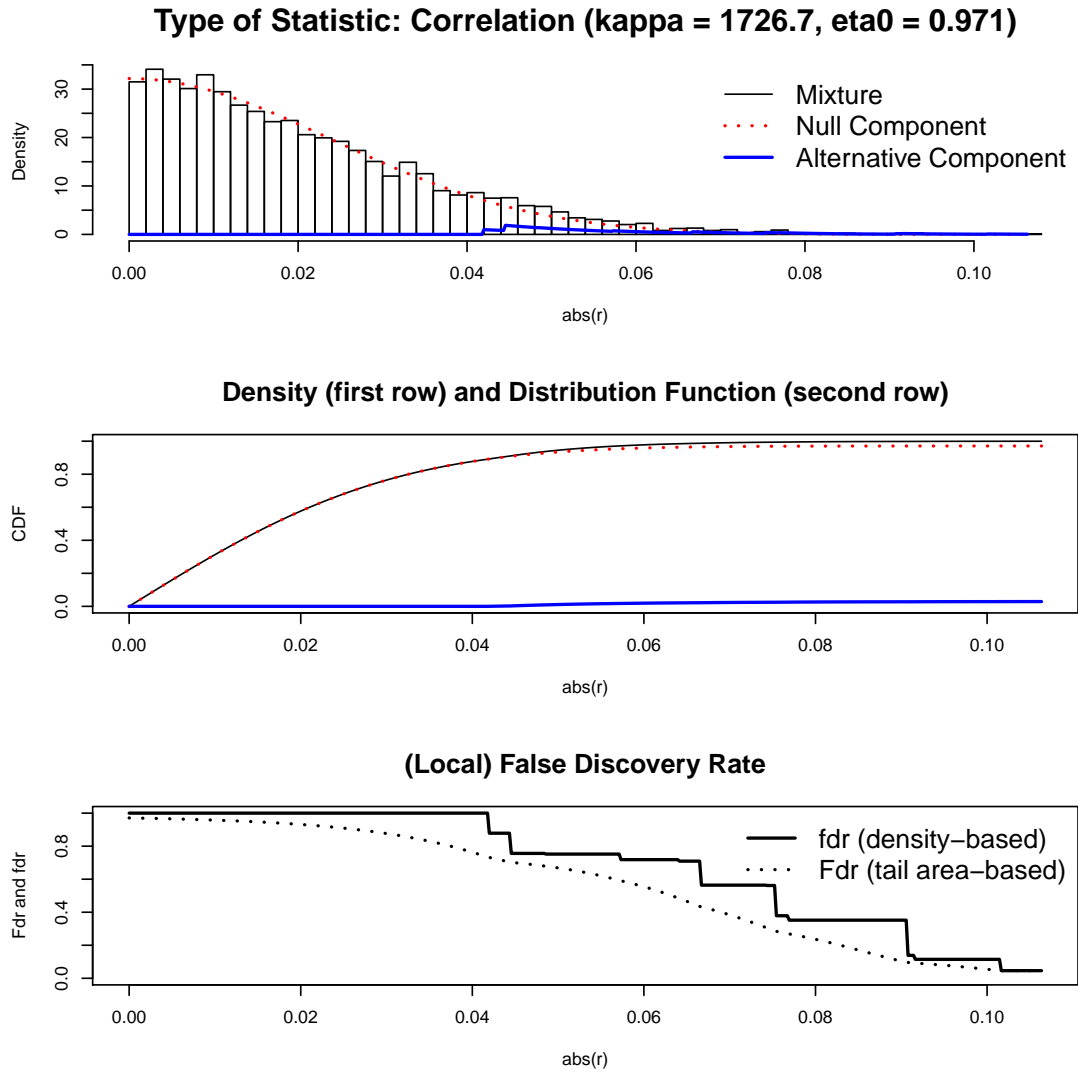


Fig. 17. Prostate Cancer model diagnostic plots of CARS scores: Density of empirical null model, cumulative distribution function and local FDR. The first two plots show that the mixture models fits the empirical distribution well.

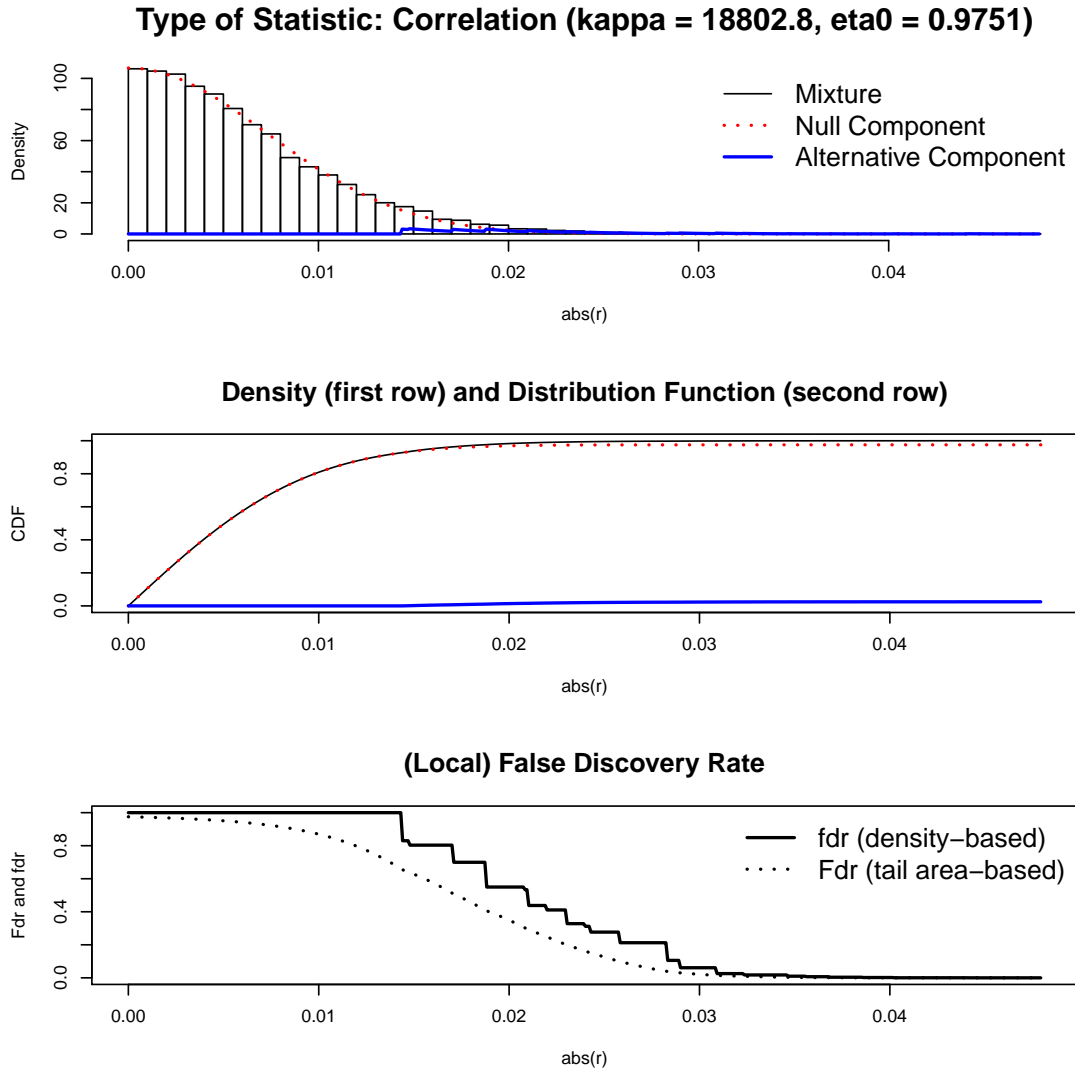


Fig. 18. Breast Cancer model diagnostic plots of CARS scores: Density of empirical null model, cumulative distribution function and local FDR. The first two plots show that the mixture models fits the empirical distribution well.

REFERENCES

- ALEXA, A., RAHNENFUHRER, J. AND LENGAUER, T. (2006). Improved scoring of functional groups from gene expression data by decorrelating go graph structure. *Bioinformatics* **22**(13), 1600–7.
- AMELIO, I., CUTRUZZOLA, F., ANTONOV, A., AGOSTINI, M. AND MELINO, G. (2014). Serine and glycine metabolism in cancer. *Trends in Biochemical Sciences* **39**(4), 191–8.
- BENJAMINI, Y. AND HOCHBERG, Y. (1995). Controlling the false discovery rate a practical and powerful approach to multiple testing. *Journal of Royal Statistical Society B* **57**(1), 289–300.
- BIBIKOVA, M., TALANTOV, D., CHUDIN, E. AND ET AL. (2004). Quantitative gene expression profiling in formalin-fixed, paraffin-embedded tissues using universal bead arrays. *The American Journal of Pathology* **165**(5), 1799–1807.
- BOEDTKJER, E., MOREIRA, J. M., MELE, M., VAHL, P., WIELENGA, V. T., CHRISTIANSEN, P. M., JENSEN, V. E., PEDERSEN, S. F. AND AALKJAER, C. (2013). Contribution of Na^+ , HCO_3^- -cotransport to cellular pH control in human breast cancer: a role for the breast cancer susceptibility locus nbcn1 (slc4a7). *International Journal of Cancer* **132**(6), 1288–99.
- BRADLOW, H. L., HERSHCOPF, R., MARTUCCI, C. AND FISHMAN, J. (1986). 16 α -hydroxylation of estradiol: a possible risk marker for breast cancer. *Annals of the New York Academy of Sciences* **464**, 138–51.
- CARROLL, R. J. AND RUPPERT, D. (1988). *Transformation and Weighting in Regression*. New York: Chapman & Hall.
- CONSORTIUM, THE GENE ONTOLOGY. (2001). Creating the gene ontology resource: Design and implementation. *Genome Research* **11**(8), 1425–1433.

- EDGAR, R., DOMRACHEV, M. AND LASH, A. E. (2002). Gene expression omnibus: NCBI gene expression and hybridization array data repository. *Nucleic Acids Research* **30**(1), 207–210.
- ELSTRODT, J. (2011). *Maß- und Integrationstheorie*. Springer.
- FAN, J. AND LV, J. (2008). Sure independence screening for ultrahigh dimensional feature space. *Journal of the Royal Statistical Society: Series B (Statistical Methodology)* **70**(5), 849–911.
- FAN, J. B., YEAKLEY, J. M., BIBIKOVA, M. AND ET AL. (2004). A versatile assay for high-throughput gene expression profiling on universal array matrices. *Genome Research* **14**(5), 878–885.
- FASIOLO, M. (2016). *An introduction to mvnfast. R package version 0.1.6..*
- GORBATENKO, A., OLESEN, C. W., BOEDTKJER, E. AND PEDERSEN, S. F. (2014). Regulation and roles of bicarbonate transporters in cancer. *Frontiers in Physiology* **5**, 130.
- GRAU, J., GROSSE, I. AND KEILWAGEN, J. (2015). PRROC: computing and visualizing precision-recall and receiver operating characteristic curves in R. *Bioinformatics* **31**(15), 2595–2597.
- GRENANDER, U. (1956). On the theory of mortality measurement. *Scandinavian Actuarial Journal* **1956**(2), 125–153.
- HATZIS, CH., PUSZTAI, L., VALERO, V. AND ET AL. (2011). A genomic predictor of response and survival following taxane-anthracycline chemotherapy for invasive breast cancer. *Journal of the American Medical Association* **305**(18), 1873–1881.
- HIGHAM, N. J. (2002). Computing the nearest correlation matrix a problem from finance. *IMA Journal of Numerical Analysis* **22**(3), 329–343.
- HORVITZ, D. G. AND THOMPSON, J. D. (1952). A generalization of sampling without replacement from a finite universe. *Journal of the American Statistical Association* **47**(260), 663–685.

- HOWLADER, N., NOONE, A.M., KRAPCHO, M. *and others*. (2016, April). Seer cancer statistics review. Website, http://seer.cancer.gov/csr/1975_2013/, Access 30.09.2016. National Cancer Institute. Bethesda, MD, 1975-2013, based on November 2015 SEER data submission.
- HUBER, P. J. (1967). The behaviour under maximum likelihood estimates under nonstandard conditions. In: *Statistics*, Volume 1. Proceedings of the Fifth Berkeley Symposium on Mathematical Statistics and Probability. pp. 221–233.
- HUBER, W., CAREY, V. J., GENTLEMAN, R. AND ET AL. (2015). Orchestrating high-throughput genomic analysis with Bioconductor. *Nature Methods* **12**(2), 115–121.
- ITOH, M., IWAMOTO, T., MATSUOKA, J. AND ET AL. (2014, Jan). Estrogen receptor (er) mrna expression and molecular subtype distribution in er-negative/progesterone receptor-positive breast cancers. *Breast Cancer Research and Treatment* **143**(2), 403–409.
- JAIN, M., NILSSON, R., SHARMA, S., MADHUSUDHAN, N., KITAMI, T., SOUZA, A. L., KAFRI, R., KIRSCHNER, M. W., CLISH, C. B. AND MOOTHA, V. K. (2012). Metabolite profiling identifies a key role for glycine in rapid cancer cell proliferation. *Science* **336**(6084), 1040–4.
- KAPLAN, E. L. AND MEIER, P. (1958). Nonparametric estimation from incomplete observations. *Journal of the American Statistical Association* **53**(282), 457–481.
- KESSY, A., LEWIN, A. AND STRIMMER, K. (2016, Dec). Optimal whitening and decorrelation. arXiv:1512.00809v4.
- KLAUS, B. AND STRIMMER, K. (2015). *fdrtool: Estimation of (Local) False Discovery Rates and Higher Criticism*. R package version 1.2.15.
- KLEIN, J. P., C. VAN HOUWELINGEN, H., IBRAHIM, J. G. AND ET AL. (2013). *Handbook of Survival Analysis*, Chapman & Hall/CRC Handbooks of Modern Statistical Methods. Taylor & Francis.

- KOLESNIKOV, N., HASTINGS, E., KEAYS, M. AND ET AL. (2014). Arrayexpress updatesimplifying data submissions. *Nucleic acids research* **43**(D1), D1113–D1116.
- LEHMANN, E. L. (1998). *Elements of Large-Sample Theory*, Springer Texts in Statistics. New York: Springer.
- MCLAUGHLIN, S. K., OLSEN, S. N., DAKE, B., DE RAEDT, T., LIM, E., BRONSON, R. T., BEROUKHIM, R., POLYAK, K., BROWN, M., KUPERWASSER, C. *and others.* (2013). The rasgap gene, rasal2, is a tumor and metastasis suppressor. *Cancer Cell* **24**(3), 365–78.
- NCBI. (2017). Database resources of the national center for biotechnology information. *Nucleic Acids Research* **45**(D1), D12–D17.
- POTAPOV, S., ADLER, W. AND SCHMID, M. (2012). *survAUC: Estimators of prediction accuracy for time-to-event data..* R package version 1.0-5.
- R CORE TEAM. (2017). *R: A Language and Environment for Statistical Computing*. R Foundation for Statistical Computing, Vienna, Austria.
- RIJSBERGEN, C. J. V. (1979). *Information Retrieval*, 2nd edition. Newton, MA, USA: Butterworth-Heinemann.
- SBONER, A., DEMICHELIS, F., CALZA, ST., PAWITAN, Y., SETLUR, SUNITA R., HOSHIDA, Y., PERNER, S., ADAMI, H. O., FALL, K., MUCCI, L. A., KANTOFF, P. W., STAMPFER, M., ANDERSSON, S. O., VARENHORST, E., JOHANSSON, J. E., GERSTEIN, M. B., GOLUB, T. R., RUBIN, M. A. *and others.* (2010). Molecular sampling of prostate cancer: a dilemma for predicting disease progression. *BMC Medical Genomics* **3**(1), 1–12.
- SCHÄFER, J. AND STRIMMER, K. (2005). A shrinkage approach to large-scale covariance matrix estimation and implications for functional genomics. *Statistical Applications in Genetics and Molecular Biology* **4**(1), 1–30.

- SIMON, N., FRIEDMAN, J., HASTIE, T. AND TIBSHIRANI, R. (2011). Regularization paths for Cox’s proportional hazards model via coordinate descent. *Journal of Statistical Software* **39**(5), 1–13.
- SKINNER, CH. AND MASON, B. (2012). Weighting in the regression analysis of survey data with a cross-national application. *Canadian Journal of Statistics* **40**(4), 697–711.
- STRIMMER, K. (2008). A unified approach to false discovery rate estimation. *BMC Bioinformatics* **9**(1), 1–14.
- THERNEAU, T. M. (2015). *A Package for Survival Analysis in S*. version 2.38.
- THOMPSON, M. (1997). *Theory of Sample Surveys*, Chapman & Hall/CRC Monographs on Statistics & Applied Probability. Chapman and Hall/CRC.
- VAN DER LAAN, M. J. AND ROBINS, J. M. (2003). *Unified Methods for Censored Longitudinal Data and Causality*, Springer Series in Statistics. Springer New York.
- WICKHAM, H. (2009). *ggplot2: Elegant Graphics for Data Analysis*. Springer-Verlag New York.
- YUAN, Y., ZHOU, Q. M., LI, B. AND ET AL. (2016, jun). A Threshold-free Prospective Prediction Accuracy Measure for Censored Time to Event Data. *ArXiv e-prints*.
- ZUBER, V., SILVA, P. D. AND STRIMMER, K. (2012, Oct). A novel algorithm for simultaneous SNP selection in high-dimensional genome-wide association studies. *BMC Bioinformatics* **13**(1), 284.
- ZUBER, V. AND STRIMMER, K. (2011). High-dimensional regression and variable selection using CAR scores. *Statistical Applications in Genetics and Molecular Biology* **10**(34), 2194–6302.